



# Topography-related controls on N<sub>2</sub>O emission and CH<sub>4</sub> uptake in a tropical rainforest catchment

Longfei Yu <sup>a,b,c,d</sup>, Jing Zhu <sup>a,e,\*</sup>, Hongli Ji <sup>f</sup>, Xiaolong Bai <sup>a,b,g</sup>, Youxing Lin <sup>a,b,g</sup>, Yiping Zhang <sup>a,b,g</sup>, Liqing Sha <sup>a,b,g</sup>, Yuntong Liu <sup>a,b,g</sup>, Qinghai Song <sup>a,b,g</sup>, Peter Dörsch <sup>h</sup>, Jan Mulder <sup>h</sup>, Wenjun Zhou <sup>a,b,g,\*</sup>

<sup>a</sup> Key Laboratory of Tropical Forest Ecology, Xishuangbanna Tropical Botanical Garden, Chinese Academy of Sciences, 666303 Mengla, Yunnan, China

<sup>b</sup> Center of Plant Ecology, Core Botanical Gardens, Chinese Academy of Sciences, 666303 Xishuangbanna, Yunnan, China

<sup>c</sup> Institute of Groundwater and Earth Sciences, Jinan University, 510632 Guangzhou, China

<sup>d</sup> Laboratory for Air Pollution & Environmental Technology, Empa, Swiss Federal Laboratories for Materials Science and Technology, Ueberlandstr. 129, CH-8600 Duebendorf, Switzerland

<sup>e</sup> Key Laboratory of Ecology of Rare and Endangered Species and Environmental Protection, Guangxi Normal University, Ministry of Education, 54004 Guilin, China

<sup>f</sup> Lushan Botanical Garden, Jiangxi Province, Chinese Academy of Sciences, 332900 Jiujiang, China

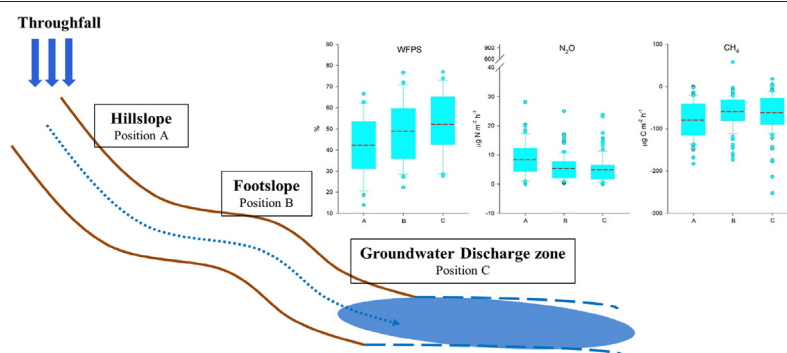
<sup>g</sup> University of Chinese Academy of Sciences, 100039 Beijing, China

<sup>h</sup> Faculty of Environmental Sciences and Natural Resource Management, Norwegian University of Life Sciences, Postbox 5003, N-1432 Aas, Norway

## HIGHLIGHTS

- Significant controls of topography on N<sub>2</sub>O and CH<sub>4</sub> fluxes in a tropical catchment
- Response of GHG fluxes to soil water contents at different topographic positions
- Weaker N<sub>2</sub>O emission and stronger CH<sub>4</sub> uptake in dry seasons
- N<sub>2</sub>O fluxes, but not CH<sub>4</sub> fluxes, respond significantly to post-drought rainfalls.

## GRAPHICAL ABSTRACT



## ARTICLE INFO

### Article history:

Received 1 December 2020

Received in revised form 29 January 2021

Accepted 29 January 2021

Available online 9 February 2021

Editor: Jay Gan

### Keywords:

Tropical rainforest

N<sub>2</sub>O emission

CH<sub>4</sub> uptake

Topography

Catchment GHG fluxes

## ABSTRACT

Forest soils in the warm-humid tropics significantly contribute to the regional greenhouse gas (GHG) budgets. However, spatial heterogeneity of GHG fluxes is often overlooked. Here, we present a study of N<sub>2</sub>O and CH<sub>4</sub> fluxes over 1.5 years, along a topographic gradient in a rainforest catchment in Xishuangbanna, SW China. From the upper hillslope to the foot of the hillslope, and further to the flat groundwater discharge zone, we observed a decrease of N<sub>2</sub>O emission associated with an increase of soil water-filled-pore-space (WFPS), which we tentatively attribute to more complete denitrification to N<sub>2</sub> at larger WFPS. In the well-drained soils on the hillslope, denitrification at anaerobic microsites or under transient water-saturation was the potential N<sub>2</sub>O source. Negative CH<sub>4</sub> fluxes across the catchment indicated a net soil CH<sub>4</sub> sink. As the oxidation of atmospheric CH<sub>4</sub> is diffusion-limited, soil CH<sub>4</sub> consumption rates were negatively related to WFPS, reflecting the topographic control. Our observations also suggest that during dry seasons N<sub>2</sub>O emission was significantly dampened (<10 μg N<sub>2</sub>O-N m<sup>-2</sup> h<sup>-1</sup>) and CH<sub>4</sub> uptake was strongly enhanced (83 μg CH<sub>4</sub>-C m<sup>-2</sup> h<sup>-1</sup>) relative to wet seasons (17 μg N<sub>2</sub>O-N m<sup>-2</sup> h<sup>-1</sup> and 56 μg CH<sub>4</sub>-C m<sup>-2</sup> h<sup>-1</sup>). In a post-drought period, several rain episodes induced exceptionally high N<sub>2</sub>O emissions (450 μg N<sub>2</sub>O-N m<sup>-2</sup> h<sup>-1</sup>) in the groundwater discharge zone, likely driven by flushing of labile organic carbon accumulated during drought. Considering the global warming potential associated with both GHGs, we found that N<sub>2</sub>O emissions largely offset the C sink contributed by CH<sub>4</sub> uptake in soils (more significant in the groundwater discharge zone). Our study illustrates important topographic controls on N<sub>2</sub>O and CH<sub>4</sub> fluxes in forest

\* Corresponding authors at: Key Laboratory of Tropical Forest Ecology, Xishuangbanna Tropical Botanical Garden, Chinese Academy of Sciences, 666303 Mengla, Yunnan, China.  
E-mail addresses: [zhuj@gxnu.edu.cn](mailto:zhuj@gxnu.edu.cn) (J. Zhu), [zhouwj@xtbg.cn.cn](mailto:zhouwj@xtbg.cn.cn) (W. Zhou).

soils. With projected climate change in the tropics, weather extremes may interact with these controls in regulating forest GHG fluxes, which should be accounted for in future studies.

© 2021 Elsevier B.V. All rights reserved.

## 1. Introduction

Nitrous oxide ( $\text{N}_2\text{O}$ ) and methane ( $\text{CH}_4$ ) are potent greenhouse gases (GHGs) with global warming potentials (over 100 years) 28 and 265 times of that of carbon dioxide ( $\text{CO}_2$ ), respectively (Myhre et al., 2013). Recent records have indicated enhanced growth of both  $\text{N}_2\text{O}$  and  $\text{CH}_4$  levels in the atmosphere (Nisbet et al., 2019; Thompson et al., 2019).  $\text{N}_2\text{O}$  and  $\text{CH}_4$  emissions may significantly offset the worldwide efforts in mitigating  $\text{CO}_2$  emissions to counteract climate change and thus challenge the Paris agreement which aims at limiting global warming to 1.5–2 °C (Millar et al., 2017). Soil emissions play a major role in global GHG budgets (Davidson and Kanter, 2014; Tian et al., 2016). Among soils with natural vegetation, warm and humid tropical forest soils are believed to be the most important  $\text{N}_2\text{O}$  source (Matson and Vitousek, 1990; Werner et al., 2007) and an active  $\text{CH}_4$  sink (Dutaur and Verchot, 2007). Globally, tropical forests are estimated to emit 1.03 Tg  $\text{N}_2\text{O}$   $\text{yr}^{-1}$  (Zhuang et al., 2012) and to take up 6.66 Tg  $\text{CH}_4$   $\text{yr}^{-1}$  (Dutaur and Verchot, 2007). However, current estimates for regional  $\text{N}_2\text{O}$  and  $\text{CH}_4$  budgets show large uncertainties, mostly due to spatial heterogeneity of GHG fluxes and limited studies of biogeochemical controls on  $\text{N}_2\text{O}$  and  $\text{CH}_4$  production/consumptions in soil (Dutaur and Verchot, 2007; Werner et al., 2007).

$\text{N}_2\text{O}$  is produced from both biotic and abiotic processes in forest soils (Butterbach-Bahl et al., 2013). Biological production of  $\text{N}_2\text{O}$  in soils generally involves nitrification and denitrification processes, which predominate in aerobic and anaerobic conditions, respectively (Weier et al., 1993). Abiotic production of  $\text{N}_2\text{O}$  occurs by chemical reactions of biological nitrogen (N) cycling intermediates (nitrite or hydroxylamine) (Liu et al., 2019), and has been shown to potentially play a role in acidic forest soils (Wei et al., 2017). Aside from production, the reduction of  $\text{N}_2\text{O}$  to  $\text{N}_2$  by denitrification is important in controlling  $\text{N}_2\text{O}$  fluxes, and this step is sensitive to oxygen availability, controlled by soil moisture (Weier et al., 1993), and to pH (Liu et al., 2010). Hence, variability of  $\text{N}_2\text{O}$  emission may be largely explained by soil carbon (C) and N substrates, temperature, moisture and soil pH. In (sub) tropical forest soils,  $\text{N}_2\text{O}$  emissions show a seasonal pattern with episodically high fluxes in the wet seasons (Zhu et al., 2013a), while the effect of soil temperature seems to be less important (Gütlein et al., 2018; Kiese et al., 2003; Kiese and Butterbach-Bahl, 2002). Lowland tropical forests usually have fast N cycling rates under warm climate, thus continuously providing inorganic N as substrate for  $\text{N}_2\text{O}$  emission (Müller et al., 2015; Vitousek and Matson, 1988). However, microbial production of  $\text{N}_2\text{O}$  in soil may depend on biologically available C and other nutrients such as phosphorus (P), which are relatively limited compared to N. Two studies which manipulated litter inputs to tropical forest soils, found that dissolved organic C derived from litter decomposition drives  $\text{N}_2\text{O}$  production through denitrification (Gao et al., 2018; Wieder et al., 2011). Other studies have applied P fertilizer to the forest floor, and observed mitigation of  $\text{N}_2\text{O}$  emissions, which they attributed to enhanced N uptake in soils (Müller et al., 2015; Yu et al., 2017b; Zheng et al., 2016).

Most well-drained forest soils constitute a net  $\text{CH}_4$  sink, i.e. take up and oxidize  $\text{CH}_4$  from atmosphere (Le Mer and Roger, 2001). High-affinity methanotrophs mediating this uptake utilize  $\text{CH}_4$  as the only C and energy source (Kolb, 2009). The activity of these methanotrophs strongly depends on the diffusion of atmospheric  $\text{CH}_4$  into soils, which is related to soil porosity (thus related to soil moisture and clay content) (Le Mer and Roger, 2001; Smith et al., 2003). By contrast, soil temperature and pH play less important roles for  $\text{CH}_4$  oxidation. In forest soils

with excessive N,  $\text{CH}_4$  uptake is often found to be inhibited (Aronson and Helliher, 2010; Kolb, 2009; Liu and Greaver, 2009). One possible mechanism is that increased  $\text{NH}_4^+$  in soil competes with  $\text{CH}_4$  for the reactive site of methane monooxygenase, the key enzyme for  $\text{CH}_4$  oxidation (Bedard and Knowles, 1989). In water-saturated forest soils, net  $\text{CH}_4$  emissions have been reported, pointing to a role of methanogenesis for net  $\text{CH}_4$  flux in forest soils under a wet climate (Itoh et al., 2009; Kaiser et al., 2018; Yu et al., 2019b). Soil  $\text{CH}_4$  production, i.e. methanogenesis, is mediated by a group of microbes (methanogens) commonly found in strictly anoxic environment (Conrad, 2009), which may become active during anoxic spells. As methanotrophs and methanogens have been reported to coexist in variable environments (Angle et al., 2017; Cai et al., 2016), both production and consumption processes need to be considered when investigating  $\text{CH}_4$  turnover, particularly in soils with fluctuating water content (Kolb and Horn, 2012).

Tropical forests are typically under warm and humid climate, thus having large potentials to become regional hotspots of GHG emissions (Hall et al., 2012; Keller et al., 1986; Werner et al., 2007). Recent studies to predict and mitigate GHG emissions associated with climatic changes and human activities in tropical forests are commonly based on climate and fertilizer manipulation experiments (Hall et al., 2012; Müller et al., 2015; Steudler et al., 2002; Werner et al., 2006), or on comparing GHG fluxes among different land-use types (Gütlein et al., 2018; Zhou et al., 2016). However, spatial heterogeneity of tropical forest soils, which is often linked with topography, has been generally overlooked when considering ecosystem-level GHG balances. Topography controls soil moisture levels, hydrological transport of nutrients and vegetation type in tropical forests, thus exerting a strong effect on forest N cycling and N gas fluxes and their responses to environmental changes (Anderson et al., 2015; Enanga et al., 2016; Weintraub et al., 2015). Fang et al. (2009) measured GHG fluxes along a steep but short slope in a broad-leaved forest of South China and found an increase of  $\text{N}_2\text{O}$  emission together with increasing soil moisture along the slope. By contrast, in a subtropical forested catchment in SW China, Zhu et al. (2013a) reported a different relationship with  $\text{N}_2\text{O}$  emissions being much larger at the upper hillslope than in a groundwater discharge zone that is occasionally water-logged. Such discrepancy may be explained by more complete denitrification to  $\text{N}_2$  in periodically submerged soils (Koehler et al., 2012) and illustrates the importance of topographic positions on N cycling and thus  $\text{N}_2\text{O}$  emission (Wexler et al., 2014; Yu et al., 2016). Previous works have also revealed topographic control on  $\text{CH}_4$  fluxes (Kaiser et al., 2018; Warner et al., 2018; Yu et al., 2019b). For example, Warner et al. (2018) identified the transition zone between upland and valley bottom as a hotspot of  $\text{CH}_4$  uptake in a temperate forests landscape. Wetland/riparian soils in the lowland subtropical-tropical forests have recently been found to be potentially important  $\text{CH}_4$  sources which could alter the ecosystem  $\text{CH}_4$  budgets (Sakabe et al., 2018).

To explore topographic controls on  $\text{N}_2\text{O}$  and  $\text{CH}_4$  fluxes in tropical rainforest catchments, we conducted in-situ measurements over 1.5 years at three topographic positions along a catchment located in SW China. This site has a pronounced monsoonal climate with distinct wet and dry seasons and provides the opportunity to examine the effect of dry-wet transition on soil-atmosphere GHG exchange (O'Connell et al., 2018). We hypothesized that: 1)  $\text{N}_2\text{O}$  emission increases and  $\text{CH}_4$  uptake decreases from the drier upper to the wetter lower topographic positions; 2) warm-humid summers promote  $\text{N}_2\text{O}$  emissions but suppress  $\text{CH}_4$  uptake; 3) topographic controls on  $\text{N}_2\text{O}$  and  $\text{CH}_4$  fluxes are less significant in the dry seasons.

## 2. Materials and methods

### 2.1. Site description

The study site is a 19.7-ha tropical forested catchment, located in Xishuangbanna (XSBN), SW China (Fig. 1). XSBN is covered by rainforests with a mean canopy height of 35 m. With a mean elevation of 750 m a.s.l., XSBN has a mean annual temperature of 21.4 °C and a mean annual precipitation of 1415 mm (Cao and Zhang, 1997). The climate shows a distinct seasonal pattern, with a cool-dry season between November and April and a warm-wet season between May and October (Fei et al., 2018). Generally, XSBN receives more than 80% of the annual precipitation during the wet season. The annual N deposition in canopy throughfall is about 10 kg ha<sup>-1</sup>. XSBN is dominated by Oxisols developed from marine sandstone (Qiao et al., 2014). XSBN soils have a thin organic layer (~1 cm), and the top-soil pH ranges from 4 to 5 (Chan et al., 2006). Organic C and total N contents in soils (0–10 cm depth) range from 24 to 28 and 1.6 to 2.8 g kg<sup>-1</sup>, respectively (Chan et al., 2006; Qiao et al., 2014).

### 2.2. Experimental design

N<sub>2</sub>O and CH<sub>4</sub> fluxes were measured at three hydrologically connected topographic positions (A, B and C) in the XSBN rainforest catchment (Fig. 1). Position A is situated at the upper hillslope, position B at the foot of the hillslope (footslope; the transition point between hillslope and groundwater discharge zone) and position C in the groundwater discharge zone near a stream. The upper hillslope is relatively steep, with an inclination of 30°. The groundwater discharge zone flattens out, and is occasionally water saturated after heavy rainfall.

From July 2013 to December 2014, we measured soil-atmosphere N<sub>2</sub>O and CH<sub>4</sub> exchange bi-weekly in triplicate plots at each of the three topographic positions. Fluxes were measured by static chambers (Yu et al., 2019b). Stainless steel frames were permanently installed in the soil weeks prior to our first sampling. During gas sampling, we used vented stainless-steel chambers (30-cm diameter and 30-cm height) deploying them against water-sealed frames. To measure fluxes,

we collected 20-ml gas samples 0, 15, 30, 45 and 60 min after chamber deployment by 50-ml syringes equipped with three-way valves. Gas samples were injected into pre-evacuated 12-ml vials crimp-sealed with butyl septa (Chromacol, UK), and transported back to the laboratory at the XSBN Tropical Botanical Garden (Chinese Academy of Sciences) where they were analyzed for N<sub>2</sub>O and CH<sub>4</sub> within 24 h. Next to each static chamber plot, we installed ceramic lysimeters (P80; Staatlich Porzellanmanufaktur, Berlin) to collect soil water from O/A and AB soil layers. Triplicates of soil water was collected bi-weekly together with the gas sampling during the wet season, but it was not possible to obtain enough soil water for chemical analysis during the dry seasons. Triplicates of water samples for each layer at each topographic position were pooled and stored at 4 °C prior to analysis.

We monitored precipitation every half an hour with a rain gauge coupled with a HOBO data logger (RG3-M, Onset, US) attached to the top of an eddy flux tower near our sampling plots. Throughfall volume was measured with a tailor-made V-shape container (2.0 m × 0.3 m and 11 replicates) installed under the forest canopy. Throughfall volume was calculated from the water levels recorded with a HOBO data logger (U20-001-04, Onset, US). At the watershed outlet, we installed a 90° V-notch weir instrumented with a water-level recorder (U20-001-04, Onset, US), which was set to take average discharge measurements at 5-min intervals. Water samples of throughfall and runoff were additionally collected bi-weekly for chemical analyses except for the period of November 2013 to January 2014. In parallel with the gas sampling, soil temperature and volumetric soil moisture were measured at 10-cm depth using a hand-held time domain reflectometer (TDR100, Campbell Scientific, Logan, Utah, USA) close to the flux sampling plots.

### 2.3. Chemical analyses and data calculation

Gas samples collected from the static chambers were analyzed for N<sub>2</sub>O and CH<sub>4</sub> mole fractions with a gas chromatograph coupled with an electron capture detector (ECD) and a flame ionization detector (FID) (Agilent GC-7890A, USA). For ECD, a makeup gas of Ar/CH<sub>4</sub> (90/10 vol%) was used. We calculated N<sub>2</sub>O and CH<sub>4</sub> fluxes by linear or polynomial regression (estimating time-zero fluxes in case a concave

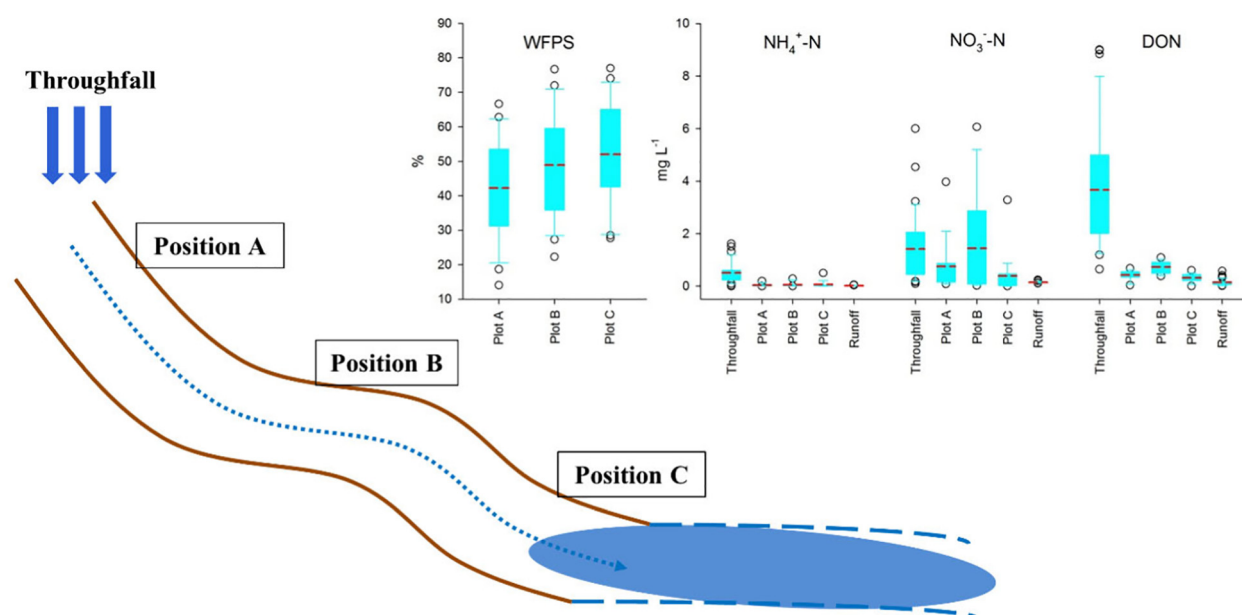


**Fig. 1.** Schematic illustration of topography and sampling locations in the studied rainforest catchment at XSBN. Plots A, B and C denote the three topographic positions upper hillslope, foot of the hillslope and groundwater discharge zone, respectively. Right insert: box and whisker plots of soil WFPS (at 10 cm depth), NH<sub>4</sub><sup>+</sup>-N and NO<sub>3</sub><sup>-</sup>-N and DON concentrations in soil water (O/A layer) measured along a hydrological continuum given by throughfall → position A → position B → position C → outlet. N concentrations were derived from measurements during the wet seasons of 2013 and 2014 only; no samples were obtained during the dry seasons. Mean values are indicated by red dashed lines.



downward curve in concentration change was seen) of gas mole fractions over time (Yu et al., 2019b; Zhu et al., 2013a).

In water samples (including precipitation, soil water and runoff), pH was measured with a pH electrode (Orion SA720, ThermoFisher, USA). We measured  $\text{NH}_4^+$  and  $\text{NO}_3^-$  concentrations in water samples with a continuous flow autoanalyzer (Auto Analyzer 3; Bran and Luebbe GmbH, Germany). Total organic carbon (TOC) and total nitrogen (TN) concentrations were determined with LiquiTOC II Elementar Analyzer System (Langensfeld, Germany). Additionally, soil water collected with lysimeter samplers had been already filtrated, so the TOC concentrations determined for soil water mostly represent dissolved organic carbon (DOC). The dissolved organic nitrogen (DON) concentration in water samples was calculated as the difference between TN and total inorganic N ( $\text{NH}_4^+$  and  $\text{NO}_3^-$ ).

We calculated soil water-filled pore space (WFPS) from the TDR-measured volumetric soil moistures (VM,  $\text{cm}^3/\text{cm}^3$ ), soil bulk density (BD,  $1.0 \text{ g}/\text{cm}^3$  for Plots A and B;  $1.2 \text{ g}/\text{cm}^3$  for Plot C) and soil particle density (PD,  $2.65 \text{ g}/\text{cm}^3$ ) (Linn and Doran, 1984) as below:

$$\text{WFPS (\%)} = \text{VM}/(1-\text{BD}/\text{PD}) * 100 \quad (1)$$

#### 2.4. Estimates of annual gas budgets

We estimated annual  $\text{N}_2\text{O}$  and  $\text{CH}_4$  fluxes based by linear interpolation of fluxes between subsequent sampling dates (Yu et al., 2019b). Annual cumulative fluxes computed for each replicate sampling plot were averaged to obtain mean annual fluxes, and uncertainties were determined as 1 SD. Considering the exceptionally high  $\text{N}_2\text{O}$  fluxes on 6/17/2014, our estimates were made by two scenarios: Scenario 1 took all flux data into account and Scenario 2 replaced fluxes on 6/17/2014 from the previous and the next samplings. To examine the combined contribution of  $\text{N}_2\text{O}$  and  $\text{CH}_4$  fluxes across three topographic positions of the XSBN catchment to global warming, we normalized the  $\text{N}_2\text{O}$  and  $\text{CH}_4$  fluxes to  $\text{CO}_2$ -equivalents ( $\text{kg CO}_2$ ) based on their global warming potentials (GWPs) (Tian et al., 2016) and calculated the net GWP contributions of three plots in the catchment as below:

$$\text{GWP}_{\text{net}} = \text{F}_{\text{N}_2\text{O}} * \text{GWP}_{\text{N}_2\text{O}} + \text{F}_{\text{CH}_4} * \text{GWP}_{\text{CH}_4} \quad (2)$$

where  $\text{GWP}_{\text{net}}$  refers to GWP contributions equivalent to  $\text{kg CO}_2 \text{ ha}^{-1} \text{ yr}^{-1}$  equivalent as a result of both  $\text{N}_2\text{O}$  and  $\text{CH}_4$  exchange;  $\text{F}_{\text{N}_2\text{O}}$  and  $\text{F}_{\text{CH}_4}$  refer to fluxes of  $\text{N}_2\text{O}$  and  $\text{CH}_4$  ( $\text{kg ha}^{-1} \text{ yr}^{-1}$ ), respectively;  $\text{GWP}_{\text{N}_2\text{O}}$  and  $\text{GWP}_{\text{CH}_4}$  refers to 100-year GWPs for  $\text{N}_2\text{O}$  (265) and  $\text{CH}_4$  (28), respectively.

#### 2.5. Statistical analyses

All statistical analyses for this study were performed with R 3.3.1 (R Core Team, 2016). We checked all data for normality (Kolmogorov-Smirnov's test) and homoscedasticity (Levene's test) before testing for statistical differences. Logarithmic or square root transformation was applied to data which were not normally distributed. We used linear mixed-effect models to test differences in  $\text{N}_2\text{O}$  and  $\text{CH}_4$  fluxes among three topographic positions (Yu et al., 2017b). For this model, we took the difference of topographic positions as a fixed effect and sampling time and replicates within each plot as random effects. We applied stepwise linear regressions of  $\text{N}_2\text{O}$  and  $\text{CH}_4$  fluxes against different biogeochemical factors. Additionally, Pearson correlation tests were applied to test individual correlations between gas fluxes and soil parameters. We used repeated analysis of variance (ANOVA) to compare soil temperature, WFPS, pH and C and N contents in soil water, and estimated annual gas budgets across topographic positions. If not specified otherwise, the level of significance is set to  $P < 0.1$ .

### 3. Results

#### 3.1. Climatic factors

From 2011 to 2015, XSBN received annual precipitation ranging from 1060 to 1419 mm (Fig. 2a). In 2014, annual precipitation declined by ~30%, indicating a drier year. If compared with the other years, 10 months in 2014 had negative rainfall anomalies which were particularly large in the cool-dry season in the beginning of 2014, suggesting drought condition (Fig. 2b). Daily precipitation and throughfall records show that most rainfall (including rainstorms) occurred in the wet seasons (May to October; Fig. 3a). By contrast, during the dry season starting from January 2014, almost no rainfall had occurred until the end of March 2014, suggesting a significant drought. The variation of runoff was generally in accordance with that of rainfall, displaying high discharge in the wet seasons (Fig. S1a).

Over the observational period of 1.5 years, temporal variation of WFPS followed that of rainfall, showing small values < 20% in March 2014 and large values up to 80% in August and September 2014. Along the topographic gradient, WFPS significantly increased in the order position  $A < B < C$  (Figs. 1 and 3a). The difference of WFPS among topographic positions was smaller in dry seasons than in wet seasons. Soil temperature at 10 cm depth was consistently  $>20^\circ\text{C}$  during the warm-wet season and varied between 15 and  $20^\circ\text{C}$  in the cool-dry season (Fig. 2b), without showing any apparent spatial pattern.

#### 3.2. Water chemistry in throughfall, runoff and soil water

Of TN in throughfall, DON concentration was highest (up to  $10 \text{ mg N L}^{-1}$ ), while  $\text{NO}_3^-$  concentration ranked second (Fig. S1b). The concentrations of TN were significantly smaller in runoff, and  $\text{NO}_3^-$  and DON contributed equally (Fig. S1c). No apparent temporal pattern of N concentrations in throughfall and runoff was found, except for elevated  $\text{NO}_3^-$  concentration in throughfall at the end of 2014 (Fig. S1b). Most likely this was due to enhanced dry deposition in the dry season of 2014, given that little rainfall occurred in this period (Fig. 3a). Furthermore, TOC concentration in throughfall spiked at the transition from dry to wet season in 2014, up to  $100 \text{ mg C L}^{-1}$  (Fig. S1b). A possible explanation is the accumulation of TOC in the canopy during the dry season without rainfall. The variations of TOC in runoff were generally in accordance with those in throughfall, but differed in magnitudes (more TOC in throughfall).

Due to drought during the dry seasons of 2013–2014, we only collected soil water from the wet seasons for chemical analyses (Figs. 4 and S2). In soil water collected from the organic horizon (O/A, Figs. 4 and 1), little  $\text{NH}_4^+$  was detected;  $\text{NO}_3^-$  and DON concentrations increased from position A to B and then decreased from position B to C. Both  $\text{NO}_3^-$  and DON concentrations were smaller in soil water than in throughfall. Significantly higher  $\text{NO}_3^-$  concentrations in soil water were found in the wet season of 2013 than in 2014 (except for position C; Fig. 4). Soil water DOC concentrations were generally higher and more variable in the wet season of 2014 than in 2013; a strong increase in DOC concentration was found at position B in the beginning of the wet season of 2014. Soil water pH, varying from 5 to 7 and was lower at position A than at down-slope topographic positions (Fig. 4), and its variability may have been largely linked with that of throughfall (Fig. S1). In soil water from the mineral horizon (AB, Fig. S2), variations of N concentration and pH were mostly similar to those found in the organic horizon. However, the  $\text{NO}_3^-$  concentration in the AB horizon was about twice as high as in the O/A horizon at positions A and B. In addition, at position C, we observed an unexpected increase of DOC concentration in the fall of 2013 in the AB horizon, but not in the O/A (Fig. S2).

#### 3.3. Spatiotemporal patterns of $\text{N}_2\text{O}$ and $\text{CH}_4$ fluxes

Comparison of linear mixed effect models fitted to  $\text{N}_2\text{O}$  fluxes at the three topographic positions indicated that  $\text{N}_2\text{O}$  emission was

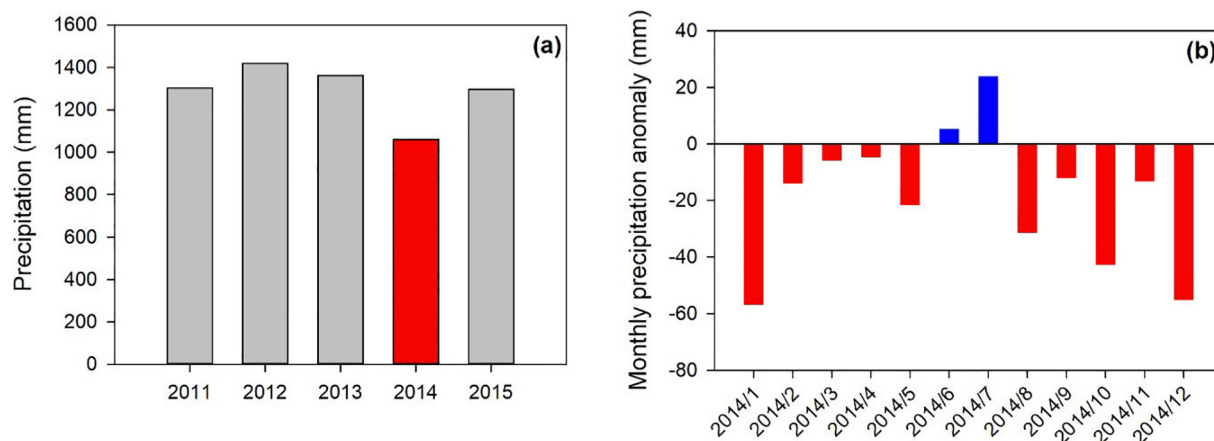


Fig. 2. **a** Annual precipitation at XSBN during 2011–2015 (the lowest value found for 2014 is marked in red). **b** Monthly precipitation anomalies in 2014 (vs. 2011–2015).

overall highest at position A (Fig. 5a). Over the entire observation period,  $\text{N}_2\text{O}$  fluxes varied from 0 to  $713 \mu\text{g N m}^{-2} \text{h}^{-1}$ , exhibiting larger variability among replicates at higher fluxes (Figs. 3c and S3). On 6/17/2014, 1.5 months after the drought period, an exceptionally high mean flux of  $450 \mu\text{g N}_2\text{O-N m}^{-2} \text{h}^{-1}$  was observed at position C. Although less pronounced, this was also seen at position B but not at A. WFPS was mostly below 50%, but several rain episodes had occurred before and at this date (70 mm in total during the week before and 30 mm on 6/17/2014), thus representing a rewetting event after drought. Emission rates of  $\text{N}_2\text{O}$  averaged for the entire observation period (as shown by box-whisker plots) decreased from the hillslope (A) to the footslope (B) and to the groundwater discharge zone (C), if the exceptionally large fluxes measured on 6/17/2014 at position C were excluded (Fig. 5a). The effect of topography on  $\text{N}_2\text{O}$  emissions became less obvious when segregated for individual seasons (Fig. 5b).  $\text{N}_2\text{O}$  emission was generally lower in the dry season than in the wet season (Fig. 5b). If compared for observations during the same months,  $\text{N}_2\text{O}$  fluxes in wet season of 2014 were larger than in 2013 at the topographic positions on the hillslope (Fig. 5c).

$\text{CH}_4$  fluxes were mostly negative, indicating that soils at the XSBN catchment acted as a sink for  $\text{CH}_4$  most of the time (Fig. 3d). According to comparison of linear mixed effect models, position A showed significantly larger  $\text{CH}_4$  uptake than positions B and C overall (Fig. 5d). When segregating  $\text{CH}_4$  fluxes for season, it can be seen that this was mainly due to very high uptake rates at position A during the dry season (Fig. 5e).  $\text{CH}_4$  uptake rates among triplicates varied between 6.3 and  $141.4 \mu\text{g C m}^{-2} \text{h}^{-1}$  and were significantly larger in the dry season than in the wet season (Fig. 5e). In the second wet season, soils took up significantly more  $\text{CH}_4$  than in the first dry season (Fig. 5f). However, on 6/17/2014 when exceptionally high  $\text{N}_2\text{O}$  fluxes were found,  $\text{CH}_4$  uptake was somewhat suppressed, but not significantly distinguishable from other fluxes recorded in the wet season of 2014 (Fig. 3d).

### 3.4. Factors controlling $\text{N}_2\text{O}$ and $\text{CH}_4$ fluxes

Stepwise linear regression including all ancillary variables (soil temperature and WFPS, soil water pH, DOC and mineral N concentrations) revealed that soil  $\text{N}_2\text{O}$  fluxes in the XSBN catchment are positively related to soil temperature and negatively related to WFPS (Table 1). By looking into individual topographic positions, we also found positive relationship between soil temperature and  $\text{N}_2\text{O}$  flux (Fig. 6a). However, at positions A and B (Fig. 6b), linear regressions showed significantly positive correlation between  $\text{N}_2\text{O}$  flux and WFPS, which is opposite to the relationship shown by stepwise

linear regression (Table 1). Pearson product-moment correlation suggested that the  $\text{N}_2\text{O}$  flux was significantly negatively correlated with soil water pH when using data from all three positions (Table S1), whereas temporal pH variability at single positions did not seem to influence  $\text{N}_2\text{O}$  flux. Such relationship may reflect the topographic control on soil water pH (wetter soils with higher pH; Figs. 4 and S2). DOC in the soil water had a significant positive effect on  $\text{N}_2\text{O}$  emissions at positions A and C but not for the entire transect (Table S1), which is in line with the results of multiple linear regression (Table 1). At position A, the  $\text{N}_2\text{O}$  flux was also significantly influenced by DON (positive) and  $\text{NH}_4^+ - \text{N}$  (negative) concentration in the soil water.

$\text{CH}_4$  fluxes across the catchment were largely (56%) explained by soil WFPS and temperature (Table 1). Positive relationships of  $\text{CH}_4$  fluxes with WFPS (i.e. a negative relationship between  $\text{CH}_4$  uptake and WFPS) and temperature were also observed at individual topographic positions (Figs. 6c&d). At position A (Table S1), Pearson correlation showed a positive effect of  $\text{NO}_3^- - \text{N}$  concentration and a negative effect of DON concentration on  $\text{CH}_4$  fluxes.

### 3.5. Annual $\text{N}_2\text{O}$ and $\text{CH}_4$ budgets

Annual  $\text{N}_2\text{O}$  fluxes across different topographic positions in the XSBN catchment varied from  $0.76$  to  $1.94 \text{ kg N ha}^{-1} \text{yr}^{-1}$ , among which the groundwater discharge zone (C) contributed the most, albeit that its uncertainty was also largest (Table 2). However, if the exceptionally high fluxes on 6/17/2014 at position C (Fig. 3c) were replaced with the averaged fluxes from the adjacent dates, the computed annual  $\text{N}_2\text{O}$  flux would be smallest ( $0.41 \text{ kg N ha}^{-1} \text{yr}^{-1}$ ).

Annual  $\text{CH}_4$  uptake rates ranged from  $5.27$  to  $7.47 \text{ kg C ha}^{-1} \text{yr}^{-1}$  and were higher at the upper hillslope (A) than at the other two topographic positions (Table 2). We calculated net global warming potential (GWP) based on the annual fluxes of  $\text{N}_2\text{O}$  and  $\text{CH}_4$ . The results suggest that soil  $\text{N}_2\text{O}$  emission at the XSBN catchment was largely offset the GWP resulting from  $\text{CH}_4$  uptake, thus turning the catchment into a net source of radiative forcing based on  $\text{N}_2\text{O}$  and  $\text{CH}_4$  which offsets the  $\text{CO}_2$  sink of this forest. Net GWP contribution increased downslope the catchment. However, if excluding the exceptionally high  $\text{N}_2\text{O}$  flux from 6/17/2014, the lower topographic positions exhibited a small sink of GWP.

## 4. Discussion

Previous catchment studies have shown that topography affects  $\text{N}_2\text{O}$  and  $\text{CH}_4$  fluxes in forest soils (Fang et al., 2009; Kaiser et al., 2018;

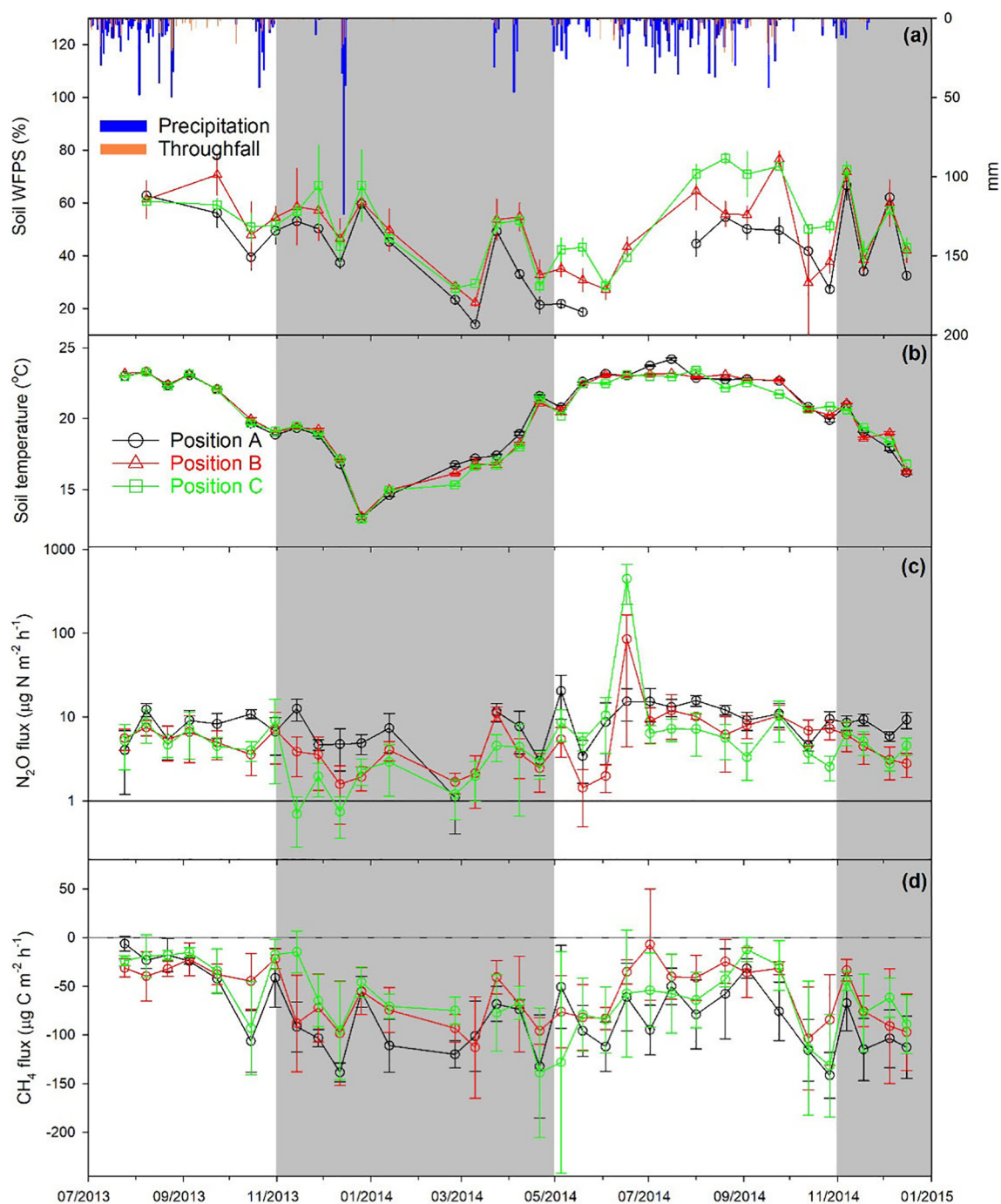


**Fig. 3.** Time-series of climatic and soil factors as well as GHG fluxes measured between July 2013 and December 2014 at topographic positions A, B and C. Panel **a** shows daily precipitation, throughfall, and soil WFPS at 10-cm depth; panel **b** shows soil temperature at 10-cm depth; panels **c** and **d** show mean  $N_2O$  and  $CH_4$  fluxes, with error bars indicating 1 SD. Note the logarithmic scale for  $N_2O$  emission rates in panel **c**. The same data plotted on a linear scale can be found in the supplement (Fig. S3). All data except precipitation were collected bi-weekly. Shaded area indicates the dry seasons.

Warner et al., 2018; Yu et al., 2019b; Zhu et al., 2013a). Our results, covering 1.5 years of  $N_2O$  and  $CH_4$  fluxes at three distinct topographic positions of the XSBN headwater catchment (Figs. 3 and 5) suggest that soil moisture gradient (Fig. 1) associated with topography is an important driver for the spatial variabilities observed for  $N_2O$  and  $CH_4$  fluxes (Fig. 6 and Table 1). At the hillslope (position A) where soils were relatively dry, we identified hotspots of both  $N_2O$  emission and  $CH_4$  uptake, while the footslope (B) and the groundwater discharge zone (C) appeared to contribute less to the  $N_2O$  source or  $CH_4$  sink, particularly during the wet season.

In non-fertilized soils,  $N_2O$  emission is often primarily associated with soil moisture content (Van Lent et al., 2015); with soil moisture contents below and near field capacity,  $N_2O$  fluxes display a positive relationship with soil moisture. At the well-drained hillslope of XSBN, where WFPS was mostly below 60%, we observed significant positive correlations of  $N_2O$  emission rates with WFPS (Figs. 6b). Both nitrification and denitrification pathways can contribute to  $N_2O$  production in soils (Firestone and Davidson, 1989), and their relative importance largely depends on oxygen availability. Positive correlation of  $N_2O$  emissions with WFPS has been taken as indicative for denitrification being

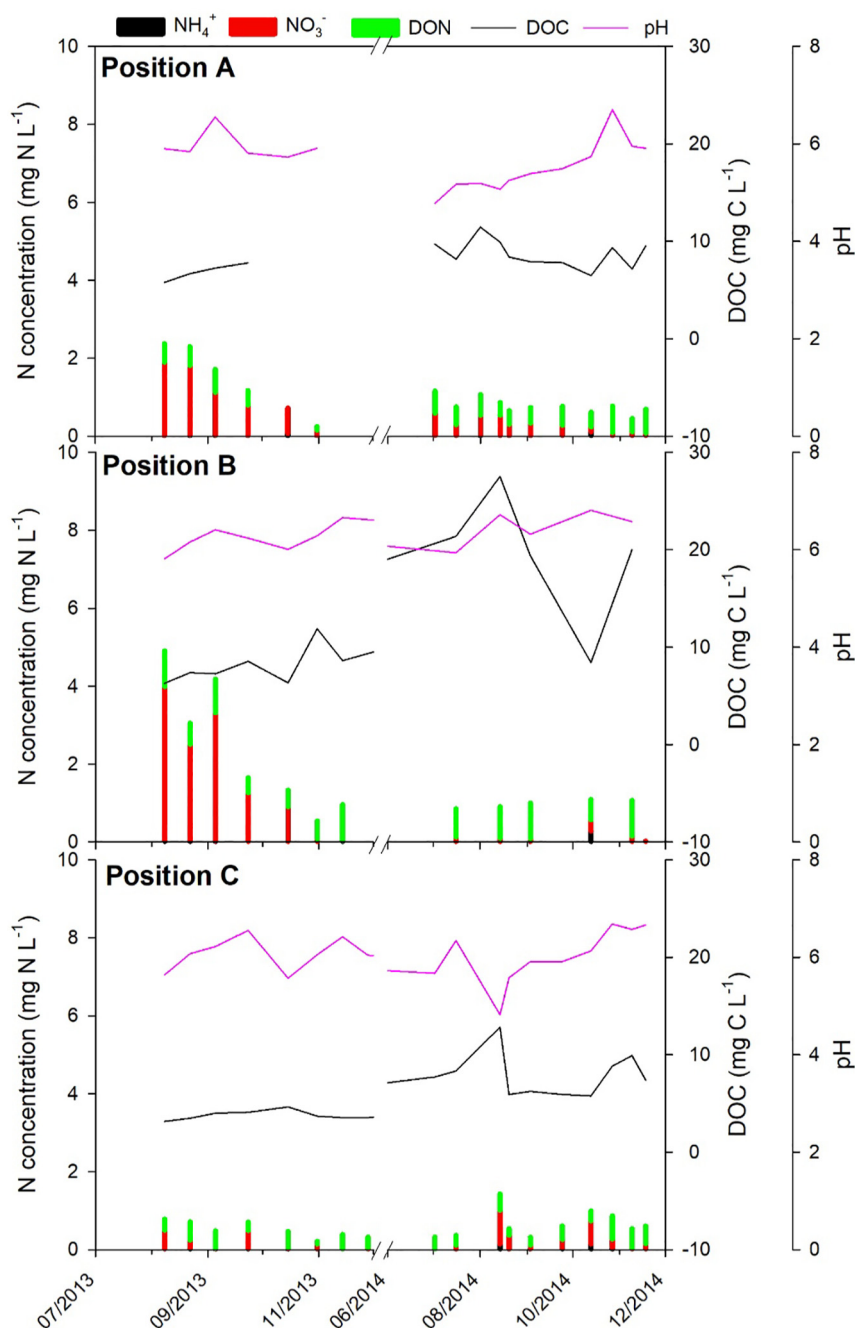


**Fig. 4.** N concentrations ( $\text{NH}_4^+$ ,  $\text{NO}_3^-$  and DON), DOC and pH of soil water sampled from the O/A horizon at three topographic positions (top panel: A; middle panel: B; bottom panel: C). In the dry seasons, the collected volumes of soil water were insufficient for chemical analyses.

the dominant source (Davidson et al., 2000). In warm and well-drained soils with abundant mineralization, however, nitrification may support denitrification directly by producing  $\text{NO}_3^-$  and indirectly by consuming oxygen at significant rates. At the hillslope of XSBN, we observed vertical increases of  $\text{NO}_3^-$  concentration within soil profiles (Figs. 4 and S2), suggesting net production of  $\text{NO}_3^-$  (i.e. nitrification). Small changes in soil moisture around 60%-WFPS may thus result in coupled nitrification-denitrification (Zhu et al., 2013a). Yu et al. (2017a) conducted a short-term in situ  $^{15}\text{N}$  tracing experiment at the hillslope in a subtropical forest in SW China and found that denitrification was the dominant  $\text{N}_2\text{O}$  source during a period with high  $\text{N}_2\text{O}$  fluxes (WFPS: 60 to 75%). At moderate WFPS values, small increases in soil moisture may stimulate nitrification, which could be a direct source of  $\text{N}_2\text{O}$ ,

particularly during the dry season at XSBN, when WFPS dropped below 40% (Fig. 3a). In addition, a short-term in situ  $^{15}\text{N}$  labeling experiment performed in the XSBN forest in late April 2016 indicated that nitrification was the predominant  $\text{N}_2\text{O}$  source during the first 27 h after adding  $^{15}\text{NO}_3^-$  (WFPS: 20 to 60%; Zhou et al., Personal Communication). However, it is beyond the scope of this study to partition  $\text{N}_2\text{O}$  sources, solely based on the gas flux and soil measurements. More field experiments with isotopic tracers covering both wet and dry seasons are needed to fully elucidate the major  $\text{N}_2\text{O}$  production processes at XSBN.

Surprisingly, opposite to our hypothesis,  $\text{N}_2\text{O}$  fluxes at the footslope and in the groundwater discharge zone, where WFPS was consistently higher, were lower than at the drier hillslope during the wet season (Figs. 3a, c and 5b). Zhu et al. (2013a) observed a similar spatial pattern



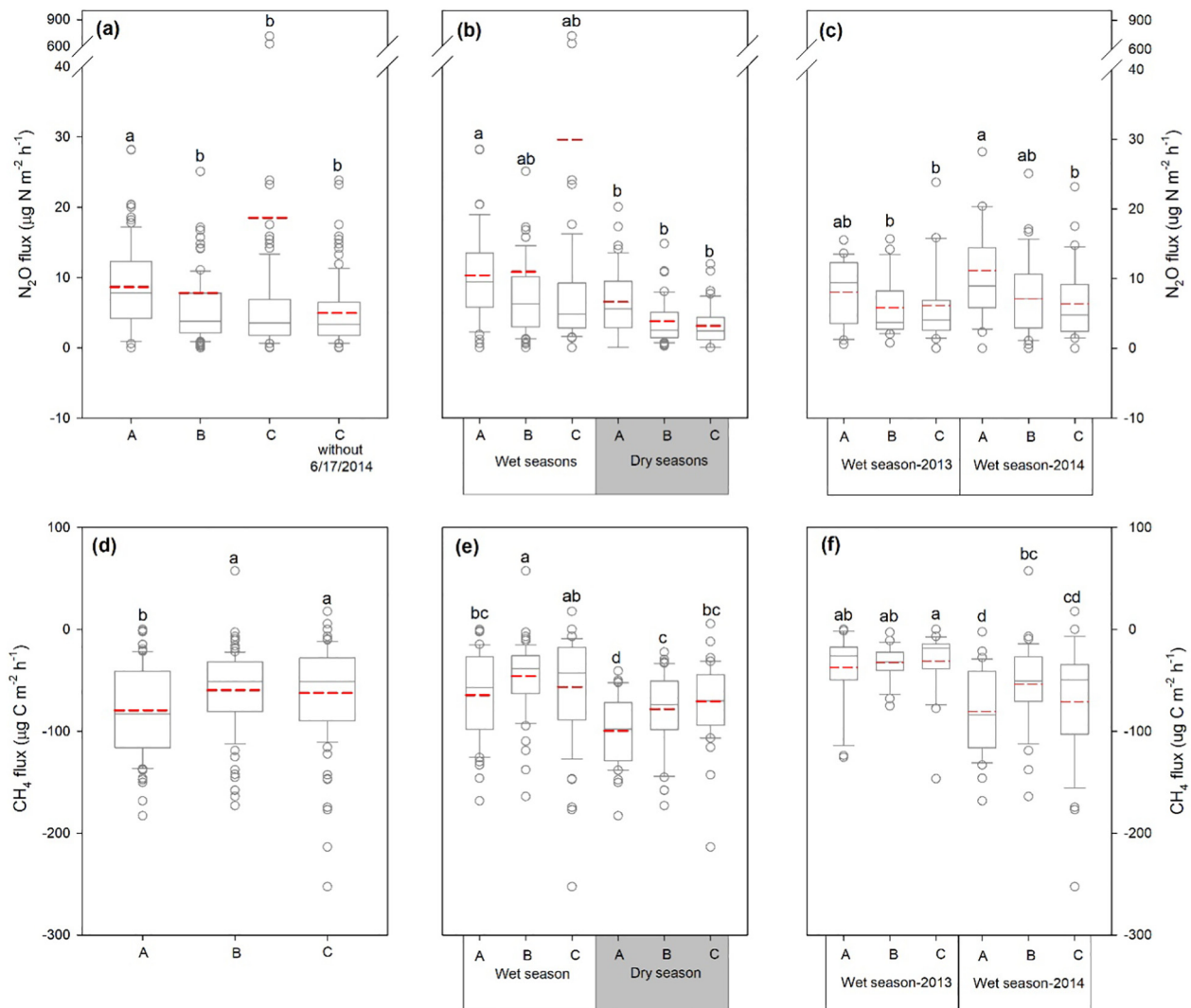


**Fig. 5.** Box and whisker plots of  $\text{N}_2\text{O}$  (a, b and c) and  $\text{CH}_4$  (d, e and f) fluxes between July 2013 and December 2014 at topographic positions A, B and C. Panels a and d compare fluxes at three topographic positions (for  $\text{N}_2\text{O}$  fluxes at C, datasets with and without the exceptional flux on 6/17/2014 were included); panels b and e compare average fluxes between wet and dry seasons; panels c and f compare fluxes between the wet seasons in 2013 and 2014 (fluxes between July and October were selected for comparison between two wet seasons, according to the availability of data). Mean values are indicated by red dash lines. Different letters indicate significant difference ( $p < 0.1$ ).

of  $\text{N}_2\text{O}$  fluxes during the wet season along a hydrological flow path in a subtropical forested catchment in SW China, showing on average lower  $\text{N}_2\text{O}$  emission rates in the wetter groundwater discharge zone than on the drier hillslope. They attributed this to lower  $\text{NO}_3^-$  availability and more complete denitrification to  $\text{N}_2$  in the more permanently saturated groundwater discharge zone, as opposed to the well-drained hillslope, which showed a flashier hydrology. Together with a significant decrease of  $\text{NO}_3^-$  in the soil solution along the hydrological flow path (Figs. 1, 4 and S2), this would support the idea that denitrifier communities in

the groundwater discharge zone express  $\text{N}_2\text{O}$  reductase more constitutively and hence have inherently lower  $\text{N}_2\text{O}/(\text{N}_2\text{O} + \text{N}_2)$  ratios. This was proven for the catchment in SW China by standardized laboratory incubations (Zhu et al., 2013b). Yu et al. (2016) later showed in situ that denitrification in the groundwater discharge zone indeed was an important N sink in this catchment. Cui et al. (2018) reported ex situ denitrification product ratios ( $\text{N}_2\text{O} / \text{N}_2\text{O} + \text{N}_2$ ) for surface soils from the XSBN catchment. Integrating over 60 h of denitrification, the  $\text{N}_2\text{O}/(\text{N}_2\text{O} + \text{N}_2)$  ratios significantly decreased from hillslope to groundwater

**Table 1**  
Stepwise linear regression of  $\text{N}_2\text{O}$  and  $\text{CH}_4$  fluxes against soil parameters<sup>a</sup>.

	Soil WFPS		Soil temperature		Equation	R <sup>2</sup> -Adjust
	Slope	p	Slope	p		
$\ln(\text{N}_2\text{O})$	-0.017	0.04	0.30	<0.01	$\ln(\text{N}_2\text{O}) = 0.30 \text{ Temp} - 0.017\text{WFPS} - 3.66$	0.35
$\text{CH}_4$	1.71	<0.01	8.30	0.03	$\text{CH}_4 = 1.71\text{WFPS} + 8.30\text{Temp} - 334$	0.56

<sup>a</sup> Soil parameters including soil WFPS and temperature (Temp), pH, DOC,  $\text{NH}_4^+\text{-N}$  and  $\text{NO}_3^-\text{-N}$  were tested for stepwise linear regression. Soil WFPS and temperature were measured at 10 cm depth. All other soil parameters were determined in the O/A layer. Parameters other than Temp and WFPS showed insignificant slopes ( $P > 0.1$ ) in the regression and were excluded during stepwise regression.



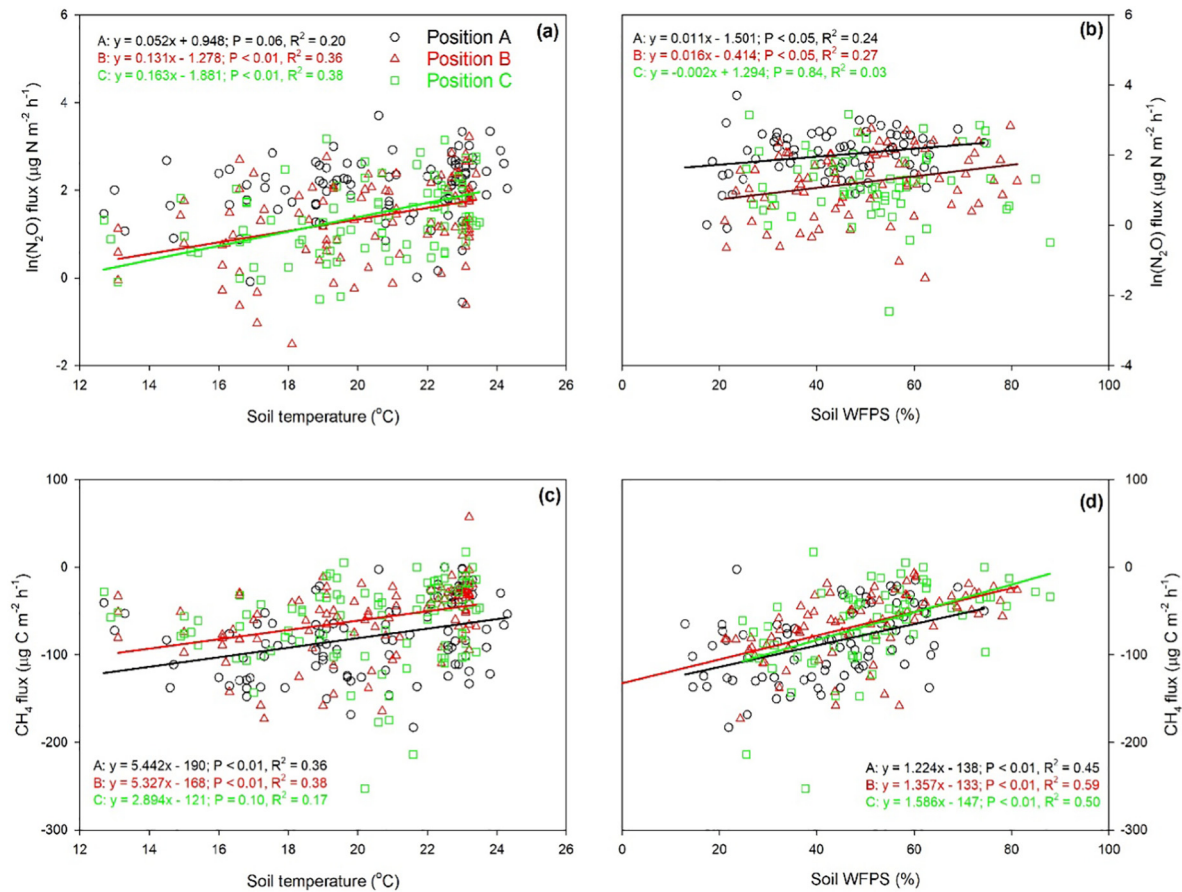


**Fig. 6.** Relationship of N<sub>2</sub>O (logarithmically transformed; sub-figures a and b) and CH<sub>4</sub> (c and d) fluxes with soil temperature and WFPS at three topographic positions along the rainforest catchment XSBN. Refer to Fig. 1 for plot codes. Soil WFPS and temperature were measured at 10 cm depth. Linear regression lines (only shown if significant;  $p < 0.1$ ) with linear polynomials are shown in each figure.

discharge zone, which was a common pattern for a number of soils from (sub)tropical forest sites in South China.

Apparent seasonal patterns of N<sub>2</sub>O fluxes were observed in all topographic positions (Figs. 3c and 5b), showing significantly higher N<sub>2</sub>O emission in the warm-wet season. Such patterns are consistent with a number of studies in the subtropics/tropics (Fang et al., 2009; Gao et al., 2018; Hall et al., 2012; Kiese et al., 2003; Zhu et al., 2013a). As shown by Table 1 and Fig. 6a&6b, both soil WFPS and temperature seemed to play roles in regulating temporal variations of N<sub>2</sub>O fluxes. However, it is difficult to disentangle their relative importance, given that soil temperature was also positively correlated with WFPS (significant for the whole

catchment and for Position C; Fig. S4). Xu-Ri et al. (2012) summarized N<sub>2</sub>O fluxes across climatic zones with a large range of temperature; their results indicated that temperature sensitivity of N<sub>2</sub>O emission is mostly apparent when comparing different climatic zones. Moreover, a number of (sub)tropical studies of N<sub>2</sub>O fluxes have reported significant impacts from soil moisture, while temperature is not a limiting factor (Gütlein et al., 2018; Kiese and Butterbach-Bahl, 2002; Tang et al., 2006; Werner et al., 2006). Therefore, we consider soil moisture as a more important driver for temporal variability of N<sub>2</sub>O emissions at XSBN.

Although mean N<sub>2</sub>O fluxes at XSBN were small ( $< 20 \mu\text{g N m}^{-2} \text{ h}^{-1}$ , Fig. S3) and not different from the mean rates from other unmanaged

**Table 2**  
Annual fluxes of N<sub>2</sub>O and CH<sub>4</sub><sup>a</sup>.

		Upper hillslope Position A		Foot of hillslope Position B		Groundwater discharge zone Position C	
		Fluxes	Uncertainty	Fluxes	Uncertainty	Fluxes	Uncertainty
Scenario 1 <sup>c</sup>	N <sub>2</sub> O (kg N ha <sup>-1</sup> yr <sup>-1</sup> )	0.76	0.07	0.71	0.59	1.94	1.25
	CH <sub>4</sub> (kg C ha <sup>-1</sup> yr <sup>-1</sup> )	-7.32 <sup>d</sup>	0.97	-5.27	1.39	-5.73	1.61
	Net GWP (equivalent to kg CO <sub>2</sub> ha <sup>-1</sup> yr <sup>-1</sup> ) <sup>b</sup>	43.2	46.5	98.9	251	594	524
Scenario 2 <sup>c</sup>	N <sub>2</sub> O (kg N ha <sup>-1</sup> yr <sup>-1</sup> )	0.75 <sup>d</sup>	0.05	0.43	0.20	0.41	0.16
	CH <sub>4</sub> (kg C ha <sup>-1</sup> yr <sup>-1</sup> )	-7.47 <sup>d</sup>	0.93	-5.31	1.49	-5.78	1.53
	Net GWP (equivalent to kg CO <sub>2</sub> ha <sup>-1</sup> yr <sup>-1</sup> ) <sup>b</sup>	33.4	40.5	-19.2	100	-45.1	87.8

<sup>a</sup> Annual budgets were estimated based on cumulative fluxes of N<sub>2</sub>O and CH<sub>4</sub> from September 2013 to August 2014. Presented fluxes are mean values computed from cumulative fluxes at triplicates, with 1 SD representing uncertainties. A, B and C refer to three topographic positions upper hillslope (A), foot of the hillslope (B) and groundwater discharge zone (C).

<sup>b</sup> Global warming potential of N<sub>2</sub>O and CH<sub>4</sub> (over 100 years) are calculated as 265 and 28 times that of CO<sub>2</sub>.

<sup>c</sup> As exceptionally high N<sub>2</sub>O fluxes occurred on 6/17/2014, N<sub>2</sub>O and CH<sub>4</sub> fluxes were computed for two scenarios, of which the first took all flux data into account and the second replaced fluxes on 6/17/2014 with the average of the previous and the following sampling. Therefore, net GWP was also computed for two scenarios.

<sup>d</sup> Significant difference among topographic positions.

soils in the tropics (Gao et al., 2018; Hall et al., 2012; Kiese et al., 2003; Werner et al., 2006), we observed exceptional peaks of  $\text{N}_2\text{O}$  emission on 6/17/2014 at the footslope and in particular in the groundwater discharge zone (Fig. 3c). Since such  $\text{N}_2\text{O}$  flux peaks were not seen in late summer 2013, the high  $\text{N}_2\text{O}$  emission rates in June 2014 may have been due to the dry-to-wet transition at the start of the rainy season. After the drought period between January and April 2014 at XSBN, several rain episodes occurred in May and June, of which the rain event on 6/17/2014 was largest (30 mm, Fig. 3a). In a water manipulation experiment in a tropical forest of Costa Rica (Nobre et al., 2001), a significant increase of soil  $\text{N}_2\text{O}$  flux was observed 8 h after a rain episode. In a review, Kim et al. (2012) found that the change of  $\text{N}_2\text{O}$  fluxes in response to soil rewetting is highest in forest ecosystems and suggested that this is due to enhanced microbial metabolism after rewetting and displacement of gas from the soil pore space through water. Furthermore, monthly precipitation anomalies in 2014 indicate that its dry season was drier while June and July were wetter than the long-term average (Fig. 2b); hence, the contrasting climatic conditions between dry and wet seasons in 2014 may explain the relatively large  $\text{N}_2\text{O}$  fluxes found in wet season 2014 compared to 2013 (Figs. 3c and 5c).

In addition to rain episodes, enhanced nutrient inputs in the post-drought period may drive high  $\text{N}_2\text{O}$  fluxes. We observed significant increases in TOC or DOC concentration in throughfall and soil water in the wet season 2014 compared with 2013 (Figs. 4 and S1b). The peak TOC concentration in throughfall in the middle March of 2014 (Fig. S1) may be due to the accumulation of organic matters in the canopy during the drought period. Therefore, we hypothesize that, at the start of wet season, accumulated organic matters from the canopy was flushed by rainfall to the soil and then transported laterally to the lower topographic positions, fueling microbial activities and thus  $\text{N}_2\text{O}$  production. Previous work has highlighted the importance of lateral nutrient transport (including  $\text{NO}_3^-$ ) along hydrological gradients driven by summer rainstorms for denitrification (Yu et al., 2019a) and  $\text{N}_2\text{O}$  emission (Enanga et al., 2016). On the other hand, studies in tropical forests have suggested that drought promotes release of organic matter to soils (e.g. root mortality) and aerobic decomposition of organic matters, which would result in more biologically available carbon in soils (Cleveland et al., 2010; Wieder et al., 2011). This is in line with the enhanced DOC availability observed in soil water at XSBN catchment after drought (Fig. 4). To confirm the importance of post-drought rewetting effects for annual  $\text{N}_2\text{O}$  budgets of tropical forest soils,  $\text{N}_2\text{O}$  emission and soil moisture would have to be measured at a higher frequency (e.g. daily; Barton et al., 2015).

The observed, predominantly negative  $\text{CH}_4$  fluxes indicate that XSBN forest soils act as a net  $\text{CH}_4$  sink (Figs. 3d and 5d).  $\text{CH}_4$  fluxes from soils depend on the balance between  $\text{CH}_4$  production by methanogens and consumption by methanotrophs (Le Mer and Roger, 2001; Smith et al., 2003). Methanotrophic activity in the aerobic surface soil horizons of XSBN surpassed  $\text{CH}_4$  production (if active) during most of the time. Net  $\text{CH}_4$  uptake decreased from the hillslope to the footslope and the groundwater discharge zone (Figs. 3d and 5d), along with increasing WFPS (Figs. 1 and 2a). Faster diffusion of atmospheric  $\text{CH}_4$  into the soil at the drier hillslope soil may have been the most important driver for the observed enhanced uptake (Veldkamp et al., 2013; Zhang et al., 2011). The strong impact of soil moisture on  $\text{CH}_4$  uptake is also reflected by the seasonal variation of  $\text{CH}_4$  fluxes, showing significantly larger  $\text{CH}_4$  uptake rates in the dry season than in the wet season (Fig. 5e). In the meanwhile, the positive correlation between soil temperature and  $\text{CH}_4$  fluxes as shown by Table 1 and Figs. 6c&6d, may rather reflect the co-variation of temperature with WFPS (Fig. S4) than indicate temperature controls on methanotrophic activity, as methanotrophs are often reported to be insensitive to temperature, especially in tropics (Le Mer and Roger, 2001). Spatiotemporal variability of methanotrophic activity may additionally be regulated by soil inorganic N (Aronson and Helliher, 2010; Kolb, 2009). For example, soil nitrifier activity could compete with methanotrophs for  $\text{O}_2$  and thus inhibit  $\text{CH}_4$  oxidation. At the

footslope, where  $\text{CH}_4$  uptake rates were smaller than at the hillslope (Fig. 5d), we observed higher  $\text{NO}_3^-$  concentrations in soil water (Figs. 1, 4 and S2), which may reflect a higher nitrification activity there. The significant negative effect of  $\text{NO}_3^-$  concentration on  $\text{CH}_4$  uptake rates at the hillslope as indicated by Pearson correlation (Table S1) supports such regulation.

The topographic gradient of  $\text{CH}_4$  fluxes observed at XSBN is similar to findings from several other studies (Itoh et al., 2009; Kaiser et al., 2018; Yu et al., 2019b). However, while previous studies reported net uptake at the higher and net emission at the lower topographic positions of the catchments, we rarely observed net  $\text{CH}_4$  emission at XSBN catchment, even in the groundwater discharge zone where WFPS was highest in the wet season (Figs. 3d and 5e). This most likely indicates inadequate anaerobiosis (non-saturated soils) and/or biologically available carbon for methanogenesis in soils (Le Mer and Roger, 2001). In other catchments reporting net  $\text{CH}_4$  sources, wetland or riparian soils with high groundwater table levels were identified (Itoh et al., 2009; Kaiser et al., 2018), which also provide biodegradable organic matter (Pacific et al., 2011) for methanogenesis. Another possible explanation is that, in the deep soils of groundwater discharge zone, most newly produced  $\text{CH}_4$  was consumed by the methanotrophs in the surface and sub soils, under fluctuations between oxic and anoxic conditions (Conrad, 2002; Kolb and Horn, 2012).

The mean  $\text{CH}_4$  sink strength over 1.5 years at the three topographic positions varied from 60 to 80  $\mu\text{g C m}^{-2} \text{ h}^{-1}$ , which is at the higher end of what is commonly reported for humid tropical forest soils (Courtois et al., 2018; Hall et al., 2012; Kiese et al., 2003; O'Connell et al., 2018; Werner et al., 2006; Wood and Silver, 2012). Highest  $\text{CH}_4$  uptake rates at XSBN were observed during the drought period (Figs. 3d and 5e). Wood and Silver (2012) excluded throughfall from a humid tropical forest soils and found that drought enhanced  $\text{CH}_4$  uptake by up to 5 times. Likewise, other studies reported significant increase in  $\text{CH}_4$  consumption during dry seasons (Kiese et al., 2003; O'Connell et al., 2018; Tang et al., 2006). In the post-drought period, one study in a humid tropical forest of Puerto Rico looked into the shifts of  $\text{CH}_4$  fluxes (O'Connell et al., 2018). They discovered a dramatic increase in net emission of  $\text{CH}_4$  from soils in all topographic positions, fueled by release of biodegradable organic matter during rewetting, which largely offset the  $\text{CH}_4$  sink from the well-drained soils during drought. Also, at our site, we observed a significant increase in DOC concentration in soil water during the post-drought period (Figs. 4 and S2). Although  $\text{N}_2\text{O}$  emissions increased noticeably (June 2014) relative to the previous wet season (Figs. 3c and 5f),  $\text{CH}_4$  fluxes did not differ from those in the previous drought period (Figs. 3d, 5e and f). It is noteworthy that WFPS in the post-drought period was always below 80% (Fig. 3b), indicating that soils in the groundwater discharge zone were not saturated during our observation. This suggests again the importance of soil water saturation for net  $\text{CH}_4$  emissions, and explains why rewetting after drought did not stimulate  $\text{CH}_4$  emission at XSBN (Fig. 3d). In addition, our observation may be explained the suppression of methanogenesis due to competition with denitrification for organic carbon in the post-drought period (Conrad, 2002; Le Mer and Roger, 2001).

We estimated annual  $\text{N}_2\text{O}$  and  $\text{CH}_4$  budgets with cumulative fluxes between September 2013 and August 2014 (Table 2) and tested two scenarios, including one considering the  $\text{N}_2\text{O}$  flux anomalies on 6/17/2014. The full dataset (Scenario 1) shows that the groundwater discharge zone contributed the highest  $\text{N}_2\text{O}$  source ( $1.94 \pm 1.25 \text{ kg N ha}^{-1} \text{ yr}^{-1}$ ) among the three topographic positions, which was largely due to the exceptionally high flux ( $450 \mu\text{g N}_2\text{O-N m}^{-2} \text{ h}^{-1}$ ) on 6/17/2014. Even though the groundwater discharge zone accounts for only <1% area of this catchment, it may be a hotspot for elevated  $\text{N}_2\text{O}$  emissions during post-drought, adding uncertainty to the catchment  $\text{N}_2\text{O}$  budget. If the flux anomalies were not considered (Scenario 2), the annual  $\text{N}_2\text{O}$  flux was largest on the hillslope. In both scenarios, there was a variable  $\text{CH}_4$  sink across different topographic positions in the catchment, ranging from 5.27 to 7.47  $\text{kg CH}_4\text{-C ha}^{-1} \text{ yr}^{-1}$  (Table 2). This  $\text{CH}_4$  sink is

clearly larger than the global average sink strength (Yu et al., 2017), which can be largely attributed to the stimulated  $\text{CH}_4$  uptake during drought, particularly in the well-drained soils of the hillslope (Figs. 3d and 5e). Considering the net GWPs associated with the two GHGs, we found that  $\text{N}_2\text{O}$  emission significantly surpassed  $\text{CH}_4$  uptake (Scenario 1, Table 2); by contrast, if  $\text{N}_2\text{O}$  flux anomalies were excluded, the  $\text{CH}_4$  sink at the lower topographic positions of the catchment would well balance the GWP of  $\text{N}_2\text{O}$  (Scenario 2, Table 2). A recent report has suggested that Yunnan region (SW China), where XSBN is located, is experiencing more extreme wet and dry events, i.e., wet seasons become wetter and dry seasons become drier (Liu et al., 2014). As a result, seasonal variations of  $\text{N}_2\text{O}$  and  $\text{CH}_4$  fluxes would be further enlarged; in wet seasons, the hillslopes which account for more than 90% of the catchment area, may act as an enhanced  $\text{N}_2\text{O}$  source with a weakened  $\text{CH}_4$  sink, while the groundwater discharge zone may contribute a notable  $\text{CH}_4$  source (Yu et al., 2019b); in dry seasons or even drought,  $\text{CH}_4$  uptake would substantially rise and  $\text{N}_2\text{O}$  emission would decline, but such C sink might be largely offset by stimulated  $\text{N}_2\text{O}$  emission in the post-drought periods (this study). Overall, as budgeted in Table 1, future climate change in this region may further stimulate  $\text{N}_2\text{O}$  emissions, and such positive contribution of GWP is unlikely to be significantly alleviated by the soil  $\text{CH}_4$  sink.

## 5. Conclusions

Observing  $\text{N}_2\text{O}$  and  $\text{CH}_4$  fluxes over 1.5 years at different landscape positions in the XSBN tropical forested catchment, we found pronounced topographic control on  $\text{N}_2\text{O}$  emissions and  $\text{CH}_4$  uptake. Hydrologically driven variability in WFPS was identified as the dominant factor controlling  $\text{N}_2\text{O}$  and  $\text{CH}_4$  fluxes, both in space and time:  $\text{N}_2\text{O}$  emission and  $\text{CH}_4$  uptake decreased significantly from the drier hillslope soils to the wetter soils in the groundwater discharge zone; by contrast, soil  $\text{N}_2\text{O}$  source was dampened in the dry season relative to the wet season while the soil  $\text{CH}_4$  sink was enhanced. In response to rain episodes, hydrological transport of labile organic carbon might have played a role in fueling episodically large post-drought  $\text{N}_2\text{O}$  emissions at the lower topographic positions of the catchment. However, such “post-drought” effects were not found for  $\text{CH}_4$  fluxes, most likely due to inadequate anoxia (low WFPS) despite rewetting. By evaluating the GWPs associated with these two GHGs, we found that the contributions from  $\text{N}_2\text{O}$  emission were significantly larger than  $\text{CH}_4$ , but the quantification of their relative importance across topographic positions requires better constraints of fluxes. With projected climate change for the tropical region in South China (Liu et al., 2014), topographic patterns of  $\text{N}_2\text{O}$  emission and  $\text{CH}_4$  consumption in tropical rainforests may be significantly altered, further adding uncertainty to regional estimates of GHG budgets.

## CRedit authorship contribution statement

J. Zhu and W. Zhou conceived this project and designed the field experiment. W. Zhou led the field sampling and laboratory analyses; H. Ji, X. Bai, Y. Lin, Y. Zhang, L. Sha, Y. Liu and Q. Song provided support during the whole sampling and data acquisition process. L. Yu, J. Zhu and W. Zhou performed data analysis and planed for the manuscript. L. Yu wrote the main manuscript; J. Zhu, W. Zhou, P. Dörsch and J. Mulder were involved in the revisions of the article. All authors were involved in the scientific discussions and commenting on the manuscript.

## Declaration of competing interest

The authors declare that they have no known competing financial interests or personal relationships that could have appeared to influence the work reported in this paper.

## Acknowledgement

This study was supported by the National Natural Science Foundation of China under Grant Numbers 42073080, 41603082, 41967005, U1602234 and 4191101289, Yunnan Province Science Foundation (2016FB073), the CAS 135 project (Grant Numbers 2017XTBG-T01 and 2017XTBG-F01), CAS Key Laboratory of Tropical Forest Ecology (09KF001B04).

LY was supported by the EMPAPOSTDOCS-II program, which receives funding from the European Union's Horizon 2020 research and innovation program under the Marie Skłodowska-Curie grant agreement number 754364. JZ received additional grants from “The Hundred-Overseas Talents Introduction Plan of Colleges and Universities in Guangxi”. JM and PD were funded by Norwegian Research Council project “Forest in South China: an important sink for reactive nitrogen and a regional hotspot for  $\text{N}_2\text{O}$ ?” (no. 209696/E10). We thank all the technicians from the Central Laboratory of XTBG, CAS, for their support with the soil and water analyses. We thank the staff members at the Xishuangbanna Station for Tropical Rainforest Ecosystem Studies and the students and the technicians from the Global Change Research for helping with field and laboratory work.

## Appendix A. Supplementary data

Supplementary data to this article can be found online at <https://doi.org/10.1016/j.scitotenv.2021.145616>.

## References

- Anderson, T.R., Groffman, P.M., Walter, M.T., 2015. Using a soil topographic index to distribute denitrification fluxes across a northeastern headwater catchment. *J. Hydrol.* 522, 123–134. <https://doi.org/10.1016/j.jhydrol.2014.12.043>.
- Angle, J.C., Morin, T.H., Solden, L.M., Narrowe, A.B., Smith, G.J., Borton, M.A., Rey-Sanchez, C., Daly, R.A., Mirfenderesgi, G., Hoyt, D.W., Riley, W.J., Miller, C.S., Bohrer, G., Wrighton, K.C., 2017. Methanogenesis in oxygenated soils is a substantial fraction of wetland methane emissions. *Nat. Commun.* 8, 1–9. <https://doi.org/10.1038/s41467-017-01753-4>.
- Aronson, E.L., Helliker, B.R., 2010. Methane flux in non-wetland soils in response to nitrogen addition: a meta-analysis. *Ecology* 91, 3242–3251. <https://doi.org/10.1890/09-2185.1>.
- Barton, L., Wolf, B., Rowlings, D., Scheer, C., Kiese, R., Grace, P., Stefanova, K., Butterbach-Bahl, K., 2015. Sampling frequency affects estimates of annual nitrous oxide fluxes. *Sci. Rep.* 5, 1–9. <https://doi.org/10.1038/srep15912>.
- Bedard, C., Knowles, R., 1989. Physiology, biochemistry, and specific inhibitors of  $\text{CH}_4$ ,  $\text{NH}_4^+$ , and CO oxidation by methanotrophs and nitrifiers. *Microbiol. Rev.* 53, 68–84.
- Butterbach-Bahl, K., Baggs, E.M., Dannenmann, M., Kiese, R., Zechmeister-Boltenstern, S., 2013. Nitrous oxide emissions from soils: how well do we understand the processes and their controls? *Philos. Trans. R. Soc. Lond. Ser. B Biol. Sci.* 368, 20130122. <https://doi.org/10.1098/rstb.2013.0122>.
- Cai, Y., Zheng, Y., Bodelier, P.L.E., Conrad, R., Jia, Z., 2016. Conventional methanotrophs are responsible for atmospheric methane oxidation in paddy soils. *Nat. Commun.* 7, 1–10. <https://doi.org/10.1038/ncomms11728>.
- Cao, M., Zhang, J., 1997. Tree species diversity of tropical forest vegetation in Xishuangbanna, SW China. *Biodivers. Conserv.* 6, 995–1006. <https://doi.org/10.1023/A:1018367630923>.
- Chan, O.C., Yang, X., Fu, Y., Feng, Z., Sha, L., Casper, P., Zou, X., 2006. 16S rRNA gene analyses of bacterial community structures in the soils of evergreen broad-leaved forests in south-west China. *FEMS Microbiol. Ecol.* 58, 247–259. <https://doi.org/10.1111/j.1574-6941.2006.00156.x>.
- Cleveland, C.C., Wieder, W.R., Reed, S.C., Townsend, A.R., 2010. Experimental drought in a tropical rain forest increases soil carbon dioxide losses to the atmosphere. *Ecology* 91, 2313–2323. <https://doi.org/10.1890/09-1582.1>.
- Conrad, R., 2002. Control of microbial methane production in wetland rice fields. *Nutr. Cycl. Agroecosystems* 64, 59–69. <https://doi.org/10.1023/A:1021178713988>.
- Conrad, R., 2009. The global methane cycle: recent advances in understanding the microbial processes involved. *Environ. Microbiol. Rep.* 1, 285–292. <https://doi.org/10.1111/j.1758-2229.2009.00038.x>.
- Courtois, E.A., Stahl, C., Van den Berge, J., Bréchet, L., Van Langenhove, L., Richter, A., Urbina, I., Soong, J.L., Peñuelas, J., Janssens, I.A., 2018. Spatial variation of soil  $\text{CO}_2$ ,  $\text{CH}_4$  and  $\text{N}_2\text{O}$  fluxes across topographical positions in tropical forests of the Guiana Shield. *Ecosystems*. <https://doi.org/10.1007/s10021-018-0232-6>.
- Cui, J., Zhu, J., Wang, Z., Mulder, J., Wang, B., Zhang, X., 2018. The regional variation of denitrification phenotypes under anoxic incubation with soils from eight forested catchments in different climate zones of China. *Sci. Total Environ.* 615, 319–329. <https://doi.org/10.1016/j.scitotenv.2017.09.251>.
- Davidson, E.A., Kanter, D., 2014. Inventories and scenarios of nitrous oxide emissions. *Environ. Res. Lett.* 9. <https://doi.org/10.1088/1748-9326/9/10/105012>.



- Davidson, E.A., Keller, M., Erickson, H.E., Verchot, L.V., Veldkamp, E., 2000. Testing a conceptual model of soil emissions of nitrous and nitric oxides. *Bioscience* 50, 667. [https://doi.org/10.1641/0006-3568\(2000\)050\[0667:TACMOS\]2.0.CO;2](https://doi.org/10.1641/0006-3568(2000)050[0667:TACMOS]2.0.CO;2).
- Dutaur, L., Verchot, L.V., 2007. A global inventory of the soil CH<sub>4</sub> sink. *Glob. Biogeochem. Cycles* 21, GB4013. <https://doi.org/10.1029/2006GB002734>.
- Enanga, E.M., Creed, I.F., Casson, N.J., Beall, F.D., 2016. Summer storms trigger soil N<sub>2</sub>O efflux episodes in forested catchments. *J. Geophys. Res. Biogeosci.* 121, 95–108. <https://doi.org/10.1002/2015JG003027>.
- Fang, Y., Gundersen, P., Zhang, W., Zhou, G., Christiansen, J.R., Mo, J., Dong, S., Zhang, T., 2009. Soil-atmosphere exchange of N<sub>2</sub>O, CO<sub>2</sub> and CH<sub>4</sub> along a slope of an evergreen broad-leaved forest in southern China. *Plant Soil* 319, 37–48. <https://doi.org/10.1007/s11104-008-9847-2>.
- Fei, X., Song, Q., Zhang, Y., Liu, Y., Sha, L., Yu, G., Zhang, L., Duan, C., Deng, Y., Wu, C., Lu, Z., Luo, K., Chen, A., Xu, K., Liu, W., Huang, H., Jin, Y., Zhou, R., Li, J., Lin, Y., Zhou, L., Fu, Y., Bai, X., Tang, X., Gao, J., Zhou, W., Grace, J., 2018. Carbon exchanges and their responses to temperature and precipitation in forest ecosystems in Yunnan, Southwest China. *Sci. Total Environ.* 616–617, 824–840. <https://doi.org/10.1016/j.scitotenv.2017.10.239>.
- Firestone, M.K., Davidson, E.A., 1989. Microbiological basis of NO and N<sub>2</sub>O production and consumption in soil. In: Andreae, M.O., Schimel, D.S. (Eds.), *Exchange of Trace Gases between Terrestrial Ecosystems and the Atmosphere*. John Wiley and Sons, New York, pp. 7–21.
- Gao, J., Zhou, W., Liu, Y., Zhu, J., Sha, L., Song, Q., Ji, H., Lin, Y., Fei, X., Bai, X., Zhang, X., Deng, Y., Deng, X., Yu, G., Zhang, J., Zheng, X., Grace, J., Zhang, Y., 2018. Effects of litter inputs on N<sub>2</sub>O emissions from a tropical rainforest in Southwest China. *Ecosystems* 21, 1013–1026. <https://doi.org/10.1007/s10021-017-0199-8>.
- Gütlein, A., Gerschlauser, F., Kikoti, I., Kiese, R., 2018. Impacts of climate and land use on N<sub>2</sub>O and CH<sub>4</sub> fluxes from tropical ecosystems in the Mt. Kilimanjaro region. *Tanzania. Glob. Chang. Biol.* 24, 1239–1255. <https://doi.org/10.1111/gcb.13944>.
- Hall, S.J., McDowell, W.H., Silver, W.L., 2012. When wet gets wetter: decoupling of moisture, redox biogeochemistry, and greenhouse gas fluxes in a humid tropical forest soil. *Ecosystems* 16, 576–589. <https://doi.org/10.1007/s10021-012-9631-2>.
- Itoh, M., Ohte, N., Koba, K., 2009. Methane flux characteristics in forest soils under an East Asian monsoon climate. *Soil Biol. Biochem.* 41, 388–395. <https://doi.org/10.1016/j.soilbio.2008.12.003>.
- Kaiser, K.E., McGlynn, B.L., Dore, J.E., 2018. Landscape analysis of soil methane flux across complex terrain. *Biogeosciences* 15, 3143–3167. <https://doi.org/10.5194/bg-2017-518>.
- Keller, M., Kaplan, W.A., and Wofsy, S.C., 1986. Emissions of N<sub>2</sub>O, CH<sub>4</sub> and CO<sub>2</sub> from tropical forest soils. *J. Geophys. Res.* 91, 11791–11802. <https://doi.org/10.1029/JD091iD11p11791>.
- Kiese, R., Butterbach-Bahl, K., 2002. N<sub>2</sub>O and CO<sub>2</sub> emissions from three different tropical forest sites in the wet tropics of Queensland, Australia. *Soil Biol. Biochem.* 34, 975–987. [https://doi.org/10.1016/S0038-0717\(02\)00031-7](https://doi.org/10.1016/S0038-0717(02)00031-7).
- Kiese, R., Hewett, B., Graham, A., Butterbach-Bahl, K., 2003. Seasonal variability of N<sub>2</sub>O emissions and CH<sub>4</sub> uptake by tropical rainforest soils of Queensland, Australia. *Global Biogeochem. Cycles* 17, 1043. <https://doi.org/10.1029/2002gb002014>.
- Kim, D.G., Vargas, R., Bond-Lamberty, B., Turetsky, M.R., 2012. Effects of soil rewetting and thawing on soil gas fluxes: a review of current literature and suggestions for future research. *Biogeosciences* 9, 2459–2483. <https://doi.org/10.5194/bg-9-2459-2012>.
- Koehler, B., Corre, M.D., Steger, K., Well, R., Zehe, E., Sueta, J.P., Veldkamp, E., 2012. An in-depth look into a tropical lowland forest soil: nitrogen-addition effects on the contents of N<sub>2</sub>O, CO<sub>2</sub> and CH<sub>4</sub> and N<sub>2</sub>O isotopic signatures down to 2-m depth. *Biogeochemistry* 111, 695–713. <https://doi.org/10.1007/s10533-012-9711-6>.
- Kolb, S., 2009. The quest for atmospheric methane oxidizers in forest soils. *Environ. Microbiol. Rep.* 1, 336–346. <https://doi.org/10.1111/j.1758-2229.2009.00047.x>.
- Kolb, S., Horn, M.A., 2012. Microbial CH<sub>4</sub> and N<sub>2</sub>O consumption in acidic wetlands. *Front. Microbiol.* 3, 1–8. <https://doi.org/10.3389/fmicb.2012.00078>.
- Le Mer, J., Roger, P., 2001. Production, oxidation, emission and consumption of methane by soils: a review. *Eur. J. Soil Biol.* 37, 25–50. [https://doi.org/10.1016/S1164-5563\(01\)01067-6](https://doi.org/10.1016/S1164-5563(01)01067-6).
- Linn, D.M., Doran, J.W., 1984. Effect of water-filled pore space on carbon dioxide and nitrous oxide production in tilled and nontilled soils. *Soil Sci. Soc. Am. J.* 48, 1267–1272. <https://doi.org/10.2136/sssaj1984.03615995004800060013x>.
- Liu, L., Greaver, T.L., 2009. A review of nitrogen enrichment effects on three biogenic GHGs: the CO<sub>2</sub> sink may be largely offset by stimulated N<sub>2</sub>O and CH<sub>4</sub> emission. *Ecol. Lett.* 12, 1103–1117. <https://doi.org/10.1111/j.1461-0248.2009.01351.x>.
- Liu, B., Mørkvad, P.T., Frostegård, A., Bakken, L.R., 2010. Denitrification gene pools, transcription and kinetics of NO, N<sub>2</sub>O and N<sub>2</sub> production as affected by soil pH. *FEMS Microbiol. Ecol.* 72, 407–417. <https://doi.org/10.1111/j.1574-6941.2010.00856.x>.
- Liu, M., Xu, X., Sun, A.Y., Wang, K., Liu, W., Zhang, X., 2014. Is southwestern China experiencing more frequent precipitation extremes? *Environ. Res. Lett.* 9, 064002. <https://doi.org/10.1088/1748-9326/9/6/064002>.
- Liu, S., Schlöter, M., Hu, R., Vereecken, H., Brüggemann, N., 2019. Hydroxylamine contributes more to abiotic N<sub>2</sub>O production in soils than nitrite. *Front. Environ. Sci.* 7, 1–10. <https://doi.org/10.3389/fenvs.2019.00047>.
- Matson, P.A., Vitousek, P.M., 1990. Ecosystem approach to a global nitrous oxide budget: processes that regulate gas emissions vary in predictable ways. *Bioscience* 40, 667–672. <https://doi.org/10.2307/1311434>.
- Millar, R.J., Fuglestad, J.S., Friedlingstein, P., Rogelj, J., Grubb, M.J., Matthews, H.D., Skeie, R.B., Forster, P.M., Frame, D.J., Allen, M.R., 2017. Emission budgets and pathways consistent with limiting warming to 1.5 °C. *Nat. Geosci.* 10, 741–747. <https://doi.org/10.1038/NGEO3031>.
- Müller, A.K., Matson, A.L., Corre, M.D., Veldkamp, E., 2015. Soil N<sub>2</sub>O fluxes along an elevation gradient of tropical montane forests under experimental nitrogen and phosphorus addition. *Front. Earth Sci.* 3, 1–12. <https://doi.org/10.3389/feart.2015.00066>.
- Myhre, G., Shindell, D., Bréon, F.-M., Collins, W., Fuglestad, J., Huang, J., Koch, D., Lamarque, J.-F., Lee, D., Mendoza, B., Nakajima, T., Robock, A., Stephens, G., Takemura, T., Zhang, H., 2013. Anthropogenic and Natural Radiative Forcing. *Climate Change 2013 The Physical Science Basis: Working Group I Contribution to the Fifth Assessment Report of the Intergovernmental Panel on Climate Change* [Stocker, T.F., D. Qin, G.-K. Plattner, M. Tignor, S.K. Allen, J. Boschung, A. Nauels, Y. Xia, V. Cambridge University Press, Cambridge, United Kingdom and New York, NY, USA. doi:<https://doi.org/10.1017/CBO9781107415324.018>].
- Nisbet, E.G., Manning, M.R., Dlugokencky, E.J., Fisher, R.E., Lowry, D., White, J.W.C., Michel, S.E., Myhre, C.L., Platt, S.M., Allen, G., Bousquet, P., Brownlow, R., Cain, M., France, J.L., Hermansen, O., Hossaini, R., Jones, A.E., Levin, I., Manning, A.C., Myhre, G., Pyle, J.A., Vaughn, B., Warwick, N.J., 2019. Very strong atmospheric methane growth in the four years 2014–2017: implications for the Paris Agreement. *Glob. Biogeochem. Cycles* 1–25. <https://doi.org/10.1029/2018gb006009>.
- Nobre, A.D., Keller, M., Crill, P.M., Harris, R.C., 2001. Short-term nitrous oxide profile dynamics and emissions response to water, nitrogen and carbon additions in two tropical soils. *Biol. Fertil. Soils* 34, 363–373. <https://doi.org/10.1007/s003740100396>.
- O'Connell, C.S., Ruan, L., Silver, W.L., 2018. Drought drives rapid shifts in tropical rainforest soil biogeochemistry and greenhouse gas emissions. *Nat. Commun.* 9, 1348. <https://doi.org/10.1038/s41467-018-03352-3>.
- Pacific, V.J., McGlynn, B.L., Riveros-Iregui, D.A., Welsch, D.L., Epstein, H.E., 2011. Landscape structure, groundwater dynamics, and soil water content influence soil respiration across riparian-hillslope transitions in the Tenderfoot Creek experimental Forest. *Montana. Hydrol. Process.* 25, 811–827. <https://doi.org/10.1002/hyp.7870>.
- Qiao, N., Schaefer, D., Blagodatskaya, E., Zou, X., Xu, X., Kuzyakov, Y., 2014. Labile carbon retention compensates for CO<sub>2</sub> released by priming in forest soils. *Glob. Chang. Biol.* 20, 1943–1954. <https://doi.org/10.1111/gcb.12458>.
- Sakabe, A., Itoh, M., Hirano, T., Kusin, K., 2018. Ecosystem-scale methane flux in tropical peat swamp forest in Indonesia. *Glob. Chang. Biol.* 1–15. <https://doi.org/10.1111/gcb.14410>.
- Smith, K. a., Ball, T., Conen, F., Dobbie, K.E., Massheder, J., Rey, a., 2003. Exchange of greenhouse gases between soil and atmosphere: interactions of soil physical factors and biological processes. *Eur. J. Soil Sci.* 54, 779–791. doi:<https://doi.org/10.1046/j.1365-2389.2003.00567.x>.
- Steudler, P. a., Garcia-Montiel, D.C., Piccolo, M.C., Neill, C., Melillo, J.M., Feigl, B.J., Cerri, C.C., 2002. Trace gas responses of tropical forest and pasture soils to N and P fertilization. *Global Biogeochem. Cycles* 16, 7–1–7–12. doi:<https://doi.org/10.1029/2001GB001394>.
- Tang, X., Liu, S., Zhou, G., Zhang, D., Zhou, C., 2006. Soil-atmospheric exchange of CO<sub>2</sub>, CH<sub>4</sub>, and N<sub>2</sub>O in three subtropical forest ecosystems in southern China. *Glob. Chang. Biol.* 12, 546–560. <https://doi.org/10.1111/j.1365-2486.2006.01109.x>.
- Team, R.C., 2016. *A language and environment for statistical computing*. R Foundation for Statistical Computing, 2015. Austria, Vienna.
- Thompson, R.L., Lassaletta, L., Patra, P.K., Wilson, C., Wells, K.C., Gressent, A., Koffi, E.N., Chipperfield, M.P., Winiwarer, W., Davidson, E.A., Tian, H., 2019. Acceleration of global N<sub>2</sub>O emissions seen from two decades of atmospheric inversion. *Nat. Clim. Chang.* <https://doi.org/10.1038/s41558-019-0613-7>.
- Tian, H., Lu, C., Ciais, P., Michalak, A.M., Canadell, J.G., Saikawa, E., Huntzinger, D.N., Gurney, K.R., Sitch, S., Zhang, B., Yang, J., Bousquet, P., Bruhwiler, L., Chen, G., Dlugokencky, E., Friedlingstein, P., Melillo, J., Pan, S., Poulter, B., Prinn, R., Saunio, M., Schwalm, C.R., Wofsy, S.C., 2016. The terrestrial biosphere as a net source of greenhouse gases to the atmosphere. *Nature* 531, 225–228. <https://doi.org/10.1038/nature16946>.
- Van Lent, J., Hergoualc'h, K., Verchot, L.V., 2015. Reviews and syntheses: soil N<sub>2</sub>O and NO emissions from land use and land-use change in the tropics and subtropics: a meta-analysis. *Biogeosciences* 12, 7299–7313. <https://doi.org/10.5194/bg-12-7299-2015>.
- Veldkamp, E., Koehler, B., Corre, M.D., 2013. Indications of nitrogen-limited methane uptake in tropical forest soils. *Biogeosciences* 10, 5367–5379. <https://doi.org/10.5194/bg-10-5367-2013>.
- Vitousek, P., Matson, P., 1988. Nitrogen transformations in a range of tropical forest soils. *Soil Biol. Biochem.* 20, 361–367. [https://doi.org/10.1016/0038-0717\(88\)90017-x](https://doi.org/10.1016/0038-0717(88)90017-x).
- Warner, D.L., Vargas, R., Seyfferth, A., Inamdar, S., 2018. Transitional slopes act as hotspots of both soil CO<sub>2</sub> emission and CH<sub>4</sub> uptake in a temperate forest landscape. *Biogeochemistry* 138, 121–135. <https://doi.org/10.1007/s10533-018-0435-0>.
- Wei, J., Amelung, W., Lehtorff, E., Schlöter, M., Vereecken, H., Brüggemann, N., 2017. N<sub>2</sub>O and NO<sub>x</sub> emissions by reactions of nitrite with soil organic matter of a Norway spruce forest. *Biogeochemistry* 132, 325–342. <https://doi.org/10.1007/s10533-017-0306-0>.
- Weier, K.L., Doran, J.W., Power, J.F., Walters, D.T., 1993. Denitrification and the dinitrogen/nitrous oxide ratio as affected by soil water, available carbon, and nitrate. *Soil Sci. Soc. Am. J.* 57, 66. <https://doi.org/10.2136/sssaj1993.03615995005700010013x>.
- Weintraub, S.R., Taylor, P.G., Porder, S., Cleveland, C.C., Asner, G.P., Townsend, A.R., 2015. Topographic controls on soil nitrogen availability in a lowland tropical forest. *Ecology* 96, 1561–1574. <https://doi.org/10.1890/14-0834.1>.
- Werner, C., Zheng, X., Tang, J., Xie, B., Liu, C., Kiese, R., Butterbach-Bahl, K., 2006. N<sub>2</sub>O, CH<sub>4</sub> and CO<sub>2</sub> emissions from seasonal tropical rainforests and a rubber plantation in Southwest China. *Plant Soil* 289, 335–353. <https://doi.org/10.1007/s11104-006-9143-y>.
- Werner, C., Butterbach-Bahl, K., Haas, E., Hickler, T., Kiese, R., 2007. A global inventory of N<sub>2</sub>O emissions from tropical rainforests using a detailed biogeochemical model. *Global Biogeochem. Cycles* 21. doi:<https://doi.org/10.1029/2006GB002909>.
- Wexler, S.K., Goodale, C.L., McGuire, K.J., Bailey, S.W., Groffman, P.M., 2014. Isotopic signals of summer denitrification in a northern hardwood forested catchment. *Proc. Natl. Acad. Sci.* 111, 16413–16418. <https://doi.org/10.1073/pnas.1404321111>.
- Wieder, W.R., Cleveland, C.C., Townsend, A.R., 2011. Throughfall exclusion and leaf litter addition drive higher rates of soil nitrous oxide emissions from a lowland wet tropical forest. *Glob. Chang. Biol.* 17, 3195–3207. <https://doi.org/10.1111/j.1365-2486.2011.02426.x>.



- Wood, T.E., Silver, W.L., 2012. Strong spatial variability in trace gas dynamics following experimental drought in a humid tropical forest. *Glob. Biogeochem. Cycles* 26, 1–12. <https://doi.org/10.1029/2010GB004014>.
- Xu-Ri, Prentice, I.C., Spahni, R., Niu, H.S., 2012. Modelling terrestrial nitrous oxide emissions and implications for climate feedback. *New Phytol.* 196, 472–488. <https://doi.org/10.1111/j.1469-8137.2012.04269.x>.
- Yu, L., Zhu, J., Mulder, J., Dörsch, P., 2016. Multiyear dual nitrate isotope signatures suggest that N-saturated subtropical forested catchments can act as robust N sinks. *Glob. Chang. Biol.* 22, 3662–3674. <https://doi.org/10.1111/gcb.13333>.
- Yu, Lijun, Huang, Y., Zhang, W., Li, T., Sun, W., 2017. Methane uptake in global forest and grassland soils from 1981 to 2010. *Sci. Total Environ.* 607–608, 1163–1172. <https://doi.org/10.1016/j.scitotenv.2017.07.082>.
- Yu, L., Kang, R., Mulder, J., Zhu, J., Dörsch, P., 2017a. Distinct fates of atmogenic  $\text{NH}_4^+$  and  $\text{NO}_3^-$  in subtropical, N-saturated forest soils. *Biogeochemistry* 133, 279–294. <https://doi.org/10.1007/s10533-017-0332-y>.
- Yu, L., Wang, Y., Zhang, X., Dörsch, P., Mulder, J., 2017b. Phosphorus addition mitigates  $\text{N}_2\text{O}$  and  $\text{CH}_4$  emissions in N-saturated subtropical forest, SW China. *Biogeosciences* 14, 3097–3109. doi:doi:10.5194/bg-14-3097-2017.
- Yu, L., Mulder, J., Zhu, J., Zhang, X., Wang, Z., Dörsch, P., 2019a. Denitrification as a major regional nitrogen sink in subtropical forest catchments: evidence from multi-site dual nitrate isotopes. *Glob. Chang. Biol.* 1765–1778. <https://doi.org/10.1111/gcb.14596>.
- Yu, L., Zhu, J., Zhang, X., Wang, Z., Dörsch, P., Mulder, J., 2019b. Humid subtropical forests constitute a net methane source: a catchment-scale study. *J. Geophys. Res. Biogeosci.* 2005, 2927–2942. <https://doi.org/10.1029/2019jg005210>.
- Zhang, T., Zhu, W., Mo, J., Liu, L., Dong, S., 2011. Increased phosphorus availability mitigates the inhibition of nitrogen deposition on  $\text{CH}_4$  uptake in an old-growth tropical forest, southern China. *Biogeosciences* 8, 2805–2813. <https://doi.org/10.5194/bg-8-2805-2011>.
- Zheng, M., Zhang, T., Liu, L., Zhu, W., Zhang, W., Mo, J., 2016. Effects of nitrogen and phosphorus additions on nitrous oxide emission in a nitrogen-rich and two nitrogen-limited tropical forests. *Biogeosciences* 13, 3503–3517. <https://doi.org/10.5194/bg-2015-552>.
- Zhou, W., Ji, H., Zhu, J., Zhang, Y., Sha, L., Liu, Y., Zhang, X., Zhao, W., Dong, Y., Bai, X., Lin, Y., Zhang, J., Zheng, X., 2016. The effects of nitrogen fertilization on  $\text{N}_2\text{O}$  emissions from a rubber plantation. *Sci. Rep.* 6, 28230. <https://doi.org/10.1038/srep28230>.
- Zhu, J., Mulder, J., Wu, L.P., Meng, X.X., Wang, Y.H., Dörsch, P., 2013a. Spatial and temporal variability of  $\text{N}_2\text{O}$  emissions in a subtropical forest catchment in China. *Biogeosciences* 10, 1309–1321. <https://doi.org/10.5194/bg-10-1309-2013>.
- Zhu, J., Mulder, J., Solheimslid, S.O., Dörsch, P., 2013b. Functional traits of denitrification in a subtropical forest catchment in China with high atmogenic N deposition. *Soil Biol. Biochem.* 57, 577–586. <https://doi.org/10.1016/j.soilbio.2012.09.017>.
- Zhuang, Q., Lu, Y., Chen, M., 2012. An inventory of global  $\text{N}_2\text{O}$  emissions from the soils of natural terrestrial ecosystems. *Atmos. Environ.* 47, 66–75. <https://doi.org/10.1016/j.atmosenv.2011.11.036>.